GEOCHEMISTRY, MINERALOGY AND BENEFICIATION OF IRONSTONE FROM BIDA BASIN, NIGERIA

BY

ATADOGA, Ochala Joshua
MTech/SPS/2017/6700

DEPARTMENT OF GEOLOGY
FEDERAL UNIVERSITY OF TECHNOLOGY
MINNA

SEPTEMBER, 2021

GEOCHEMISTRY, MINERALOGY AND BENEFICIATION OF IRONSTONE FROM BIDA BASIN, NIGERIA

BY

ATADOGA, Ochala Joshua
MTech/SPS/2017/6700

A THESIS SUBMITTED TO THE POSTGRADUATE SCHOOL OF FEDERAL UNIVERSITY OF TECHNOLOGY, MINNA, NIGERIA IN PARTIAL FULFILMENT OF THE REQUIREMENTS FOR THE AWARD OF THE DEGREE OF MASTERS OF TECHNOLOGY IN GEOLOGY

(MINERAL EXPLORATION)

SEPTEMBER, 2021

ABSTRACT

The Bida Basin is a NW-SE trending inland sedimentary basin in North Central Nigeria that extends from Kontagora in the north to slightly beyond Lokoja in the south and its mesas consist of ironstone layers from which economic iron ore can be won. The stratigraphic succession in the basin comprises the Bida sandstone at the base in the northern part of the basin followed successively upward by the Sakpe, Enagi and Batati formations. The geochemistry, mineralogy and beneficiation study of the ironstone samples from the study area in the northern Bida Basin were studied. Twelve representative samples from the study area were analysed for their elemental content and three samples for mineralogical characteristics using X-ray Fluoresce(XRF) and X-ray diffraction (XRD) techniques respectively while, beneficiation study was carried out on six (6) selected samples using magnetic separation technique. The result of the chemical analysis reveals that the following oxide with their indicated average values are present in the iron ore samples; SiO_2 (24.64%), Al_2O_3 (2.24%), MnO (0.66%), CaO (0.086%), V_2O_5 (0.03%), P_2O_5 (0.03%) and Fe_2O_3(64.05%). From the XRD analysis, the dominant iron bearing mineral is the hematite which account for 71%, followed by quartz which is 21% while magnetite is 8% as the lowest mineral. The recovered iron content of the beneficiated samples ranges from 59.11% to 66.88% with an average of 62.99%. On the basis of the total iron content contained in the iron samples, a grade of 44.79% was determined which put the analyzed iron ore in a low grade class. From the discrimination plot, the analyzed ironstone plotted within the submarine –hydrothermal deposit and magnetite- silicate facies.

TABLE OF CONTENTS

CHAPTER TWO

CHAPTER THREE

LIST OF TABLES

LIST OF FIGURES

LIST OF PLATES

CHAPTER ONE

1.0 INTRODUCTION

1.1 Background to the Study

The most commonly used iron-bearing minerals contain iron compounds as follows: hematite, Fe_2O_3 (70% Fe), magnetite, Fe_3O_4 (72.4% Fe) and of much less importance are: limonite, $2Fe_2O_3.3H_2O$ (60% Fe), siderite, $FeCO_3$ (48.3% Fe); pyrite FeS_2 (46.6% Fe). These iron percentages are in their pure state.

In ores, the Fe content is lowered according to the amount of impurities present. Overall, the quality of iron ore is mainly judged based on the Fe content. More specifically, ores with Fe content above 65% are regarded as high-grade ores; 62-64% medium (or average) grade ores and those below 58% Fe are considered as low-grade ores.

Iron ore consumption for steelmaking was standing at 850million tonnes at the end of the twentieth century and was estimated to reach more than 1.3billion tonnes over the first quarter of the century (Katrak, 2008).The known world resources of crude iron ores are approximately 800billion tonnes containing about 230billion tonnes of Fe (Pollard, 2000). It is apparent that most of the known deposits contain low-grade ores with iron contents less than 30%. By contemporary growth the world consumption of iron ore (about 10% per year), the known resources of iron ores could run out within the next 64years. It is thus imperative to find new sources of iron ores to supplement the existing sources, in order to meet the growing demand. Therefore, revealing and exploiting new deposits of iron ores, particularly of high-grade is very important.

Iron constitutes 5% of the Earth's crust, making it the fourth most abundant element. Iron oxides and hydroxides form the principal iron ore minerals, due to their high iron content and occurrence as large tonnage surface deposits. Almost 300 minerals contain some iron, but only a few are considered to be important ore minerals (Table 1). Nearly all of the mined iron ore (98%) is used in iron and steel production.

Table 1: Properties of Iron minerals

Mineral	**Mineral Composition**	**%Fe (Max)**	**Specific Gravity**	**Hardness**
Hematite	Fe_2O_3	70	5.1	5-6
Magnetite	Fe_2O_3	72	5.2	5.5-6
Goethite	$Fe_2O_3.H_2O$	63	4.3	5-5.5
Lepidocrocite	$_y$-$Fe_2O_3.H_2O$	60	4.1	5
Limonite	Fe (OH).nH_2O	60	3-4	5-5.5
Siderite	$FeCO_3$	48	4.0	4
Pyrite	FeS_2	46	4.9	3
Chamosite	$(Fe_2MgAl)_5$ $(Si,Al)_4$ $O_{14}(OH)_8$	42	3.1	3
Greenalite	$Fe_3Si_2O_5(OH)_4$	45	2.9	6-6.5

Iron is a tough, malleable, magnetic metal and forms important alloys with silicon, manganese, chromium, molybdenum, titanium, aluminium, carbon, nickel and tungsten to enable manufacture of a great variety of useful metal products (Sully, 1987). Steel, an alloy of iron and carbon, is the dominant metal commodity due to its unsurpassed versatility, relatively low production cost and availability of raw materials. Iron is also used in gas and water purification systems and in the manufacture of magnets, pigments (example; ochre), abrasive (for example; magnetite as a dense medium in coal washing) and high density concrete.

Iron ore may be defined as a natural material of suitable grade, composition and physical quality that can be mined and processed for profit or economic benefit (Gross, 1993).

Iron ore deposits are widespread and have formed in a range of geological environments throughout geological time. Pratt (1993) has divided iron ore deposits into four major categories based on their mode of origin, using aspects of pervious classification by Gross (1970) and Klemic *et al* (1973).

1. Sedimentary (Banded iron formation, oolitic, placer, swamp)
2. Igneous (magmatic segregations and skarn)
3. Hydrothermal (proximal and distal)
4. Surficial enrichment (laterite and surpergene)

1.1.1 Sedimentary Deposit

Sedimentary deposits, particularly those in Banded Iron Formation (BIF), contain the bulk of the world's iron recourses. Sedimentary iron formations generally form in a variety of marine environments and rarely in continental environment (Kimberely 1989). (BIF)-hosted deposits are almost exclusively of Precambrian age and distributed worldwide. An extensive body of data indicates that BIFs form by volcanogenic or hydrothermal effusive process (Gross 1993), but the origin of BIF-derived iron ore deposits is still debated widely (Morris 1988) and (Powell *et al.,* 1999). The most recent publications on the Hamersely deposits suggested that post-depositional hydrothermal enrichment processes played a significant role in the formation of high-grade hematite ore bodies (Barlay *et al.*,1999) and (Taylor *et al.,* 2001). BIF are classified into two types ; The superior-type which formed in a near-shore continental shelf environment in type, which are associated with dolomite, quartzite and shale, and Algoma type, which are associated with volcanic (Edwards *et al.,*1986).

Oolitic deposits are Proterozoic to cretaceous in age and were an important source of iron ore before 1970. They are lower in grade (30-50% Fe) relative to BIF-hosted deposits (55-65% Fe). Two types have been identified; the Clinton type consists of deep red to purple ores composed of hematite, chamosite and siderite the Minette-type consists of brownish to dark greenish-brown ores composed mainly of siderite and iron silicate (berthieriene and chamosite). These deposit formed in shallow marine environments and accumulated along passive continental margins during times of quiescence, extension and global sea level change (Van Houten *et al.,* 1990).

1.1.2 Igneous Deposit

Igneous deposits are formed either by magmatic segregation of an immiscible magnetic rich melt in association with layered mafic-ultramafic inclusions or by injection of magnetite-rich fluids into surrounding rocks (example; Fe skarns). The former occur as massive cumulate-textured seams and are often mined for their economic concentrations of titanium and vanadium (e.g. Bushveld complex, South Africa). Fe skarns (or pyrimetasometic) are mainly derived from granitic to mafic intrusive and can be hosted in a variety of rock types. These deposits are massive irregularly shaped tabular bodies that continue to be a source of iron ore in some countries (e.g. Peru and Russia).

1.1.3 Hydrothermal Deposits

Hydrothermal iron ore deposits are formed by the circulation of heated, iron-rich aqueous solutions of magmatic, metamorphic or sedimentary parentage. These deposits form the basis of the most iron oxide copper gold (IOCG) style deposit (Hitzman *et al*., 1992). Proximal hydrothermal deposits (also known as volcanic hosted magnetic deposit) are essentially magnetite-hematite bodies that have replaced non-ferruginous host rocks (example; Kiruna iron ores). These deposit usually have obvious magmatic signature and adjacent wall rocks are generally intensely altered (Pollard 2000). Hematite bearing quartz veins within fault zones are also part of this group. Distal hydrothermal deposits are tabular to podiform stratabounds specular hematite-magnetite bodies that formed by the enrichment of an iron-rich protolith.

1.1.4 Surficial Enrichment

Surficial enrichment of iron ore deposits result from subaerial weathering process of generally low-grade ferruginous protore, commonly BIF. Mature laterites develop under a wet tropical climate and can form extensive duricrust horizons (ferricrete), rich in iron oxyhydroxides. Supergene enrichment of low-grade iron deposits essentially leaches silica and other deleterious constituents and concentrates the iron oxide minerals to produce high-grade ore that can be directly shipped. Fine earthly hematite and iron oxyhydroxides such as goethite, limonite, and lepidocrocite are the principal iron minerals produced from surface and near surface enrichment processes.

This classification system is a useful guide but transitions exists between groups and most deposits have undergone more than one Fe enchainment phase. Many BIF-hosted deposits have undergone varying degrees of hydrothermal and supergene enrichment/alteration so as to produce high-grade ore (>60% Fe). The importance of surficial enrichment (Pratt 1993) has been overshadowed by recent studies on some iron ore province which suggested that enrichment of BIF is largely due to the activity of tectonically-induced hydrothermal brines (Taylor *et al.,* 2001).

1.4 Statement of the Research

This research will provide important background on the geology, geochemistry and beneficiation processes to the recovery of the iron content in the ironstone.

It will form a crucial part in assisting the government interest in the development of the metrological sector of the economy and provide a platform for further research.

1.5 Justification of the Research

A consultant geologist Oyewola .O. In 2019 reported that Nigeria can earn about 860 billion annually from its iron ore deposit during a sensitisation forum on the opportunity in solid mineral sector**.** To sustain the meteorological industry in Nigeria, the source of raw material must not be restricted to the iron ore in Itakpe deposit but also explore the ironstone in the various part of the country. Their percentage content and beneficiation method must be established.

The stratigraphy of the ironstone in Bida Basin is well known, some researchers also analyse the mineralogical content but the beneficiation of the iron content is yet to be proven. Taylor et al., 2001 described the ironstone at Jima in Northern Bida Basin to be high grade ore or with an average of 58.86 wt.

This research will therefore investigate the geochemical, mineralogical of the ironstone with emphasis on the beneficiation of the iron content to determine the recovery content of ironstone.

1.6 Aim and Objectives of the Research

The aim of this research is to study the geochemical characteristics and processibility of the ironstone from the study area.

The objectives of the study include;

1. Field work for location of ironstone beds and their sampling.
2. Geochemical analysis of the ironstone to unravel the geochemistry and processibility.
3. Determine possible beneficiation processes to recover the iron content in the ironstone

1.7 Scope of the Research

The scope of this research is to analyse the percentage composition of the ironstone in central part of Bida Basin and to determine what percentage of the metal content that can be recovered from the ironstone in order to determine its industrial application.

1.8 Location and Accessibility of the Study Area

The field study was carried out in part of central Bida Basin from Doko to Kutigi and along Lemu Road on latitude N $08^0\,56'\,43''$ to N $09^0\,12'\,02''$ and longitude E $05^0\,57'\,26''$ to E $05^0\,36'04''$. The area is easily accessible through Minna-Bida Mokwa road. The area is well expose during dry season when grasses are usually dry.

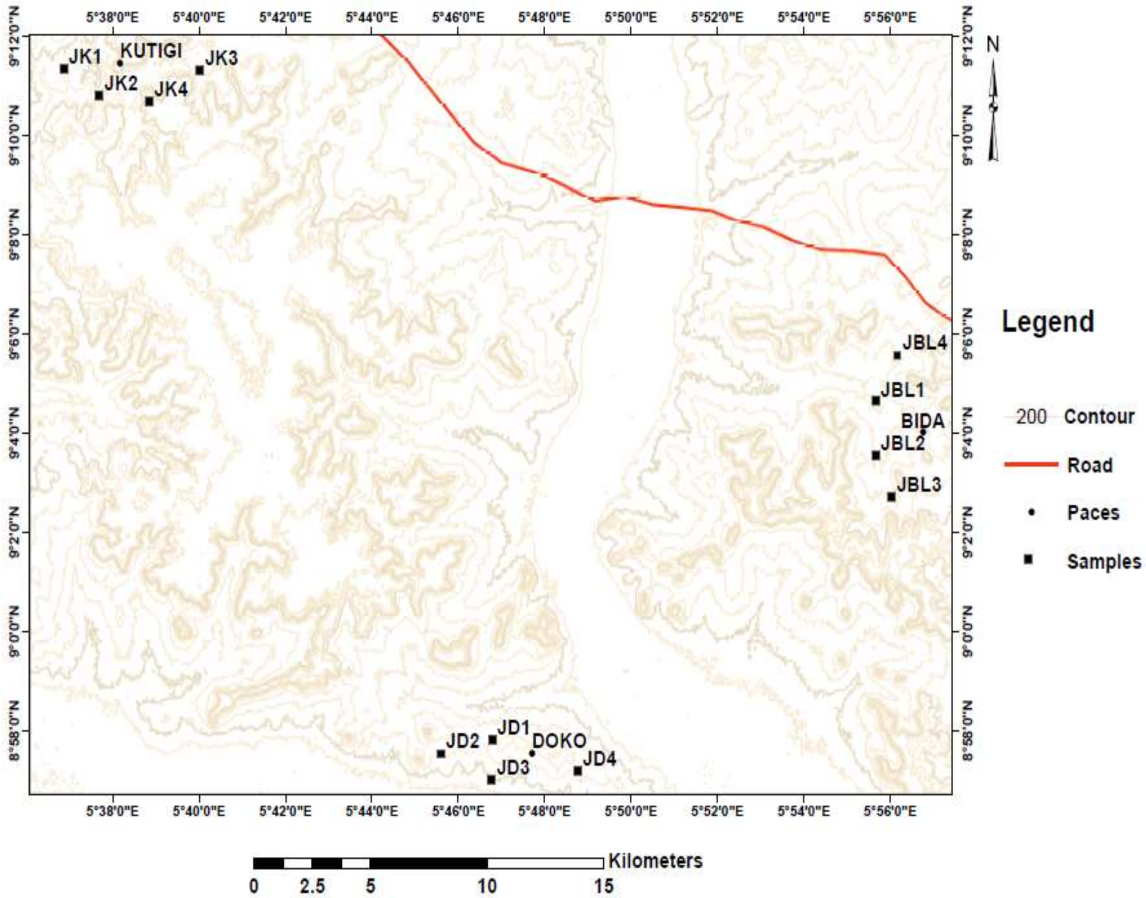

Figure 1: Location map of study area

1.9 Climate and Vegetation

The climate of Niger state is like much of West Africa. The daylight temperatures vary from 24^{oc} the middle of the wet season to above 35^{o}C at the peak of dry season. The seasonal rainfall regime gives rise to a longer wet season of about seven months with average rainfall of 250mm and a dry season of about five months with little or no rains at all. The climate is basically controlled by interaction of two widely different air masses as well as the movement of the zone of convergence of those air masses (known as the inter-tropical convergence zone ITCZ) relative to the ground. Dry season occurs between the month of November and March while the wet or rainy season runs from around April to October. The dry season is characterized by a high day time temperature of about 35^{o}C, prominent north east wind and virtually no rainfall. As a result of the seasonal rainfall regime of the study area, there is a longer wet rainy season of about seven months with an average rainfall of 250mm and a short dry season of five months with little or no rainfall. The vegetation is characterized by grasses, shrubs and trees which makes it falls under the guinea savannah of Nigeria. The vegetation tends to be thicker along the river channels with concentration of mango and other tress.

CHAPTER TWO

1.0 LITERATURE REVIEW

2.1 Introduction

The Bida Basin is a NW-SE trending intracratonic sedimentary basin extending from Kontagora in Niger state of Nigeria to areas slightly beyond Lokoja in the south. It is delimited in the northeast and southwest by the basement complex while it merges with Anambra and Sokoto Basin in sedimentary fill comprising post orogenic molasse facies and few thin unfolded marine sediments. The basin is a gently down warped trough whose genesis maybe closely connected with the santonian orogenic movements of south-eastern Nigeria and the Benue valley, nearby. The basin is a NW-SE trending embayment, perpendicular to the main axis of the Benue Trough and Niger Delta Basin. It is frequency regarded as the north-western extension of the Anambra Basin, both of which were major depocentres during the third major transgressive cycle of southern Nigeria in Late cretaceous time. Interpretations of Landsat images, borehole logs as well as geophysical data across the entire Bida Basin suggest that the basin is bounded by a system of linear faults trending NW-SE. Gravity studies also confirm central positive anomalies flanked by negative anomalies as shown for the adjacent Benue Trough and typical of rift structure (Ojo, 1984; Ojo & Ajakaiye, 1989). The Benue Trough is a failed arm of a triple junction caulacogen that existed beneath the present position of the Niger Delta during the createaceous time. The trough is filled with over 500m of predominantly Aptian to Maastrichtian sediments in the lower, middle and upper Benue geographical regions. The lower Benue Trough which includes the Anambra Basin is considered as the southern extension of the Bida Basin. Initial gravity studies in the Bida Basin put the maximum thickness of the sedimentary succession at about 3.5km (Ojo, 1984) in the central axis.

2.1.1 Stratigraphy and Sedimentation of Bida Basin

The stratigraphic succession of Bida Basin, collectively referred to as the Nupe Group (Adeleye, 1974) comprises a twofold Northern Bida Basin (sub-Basin) and southern Bidan sub-Basin or Lokoja sub-Basin. The basin fill comprises a northwest trending belt of upper cretaceous sedimentary rocks that were deposited as a result of block faulting, basement fragmentation subsidence rifting and drifting consequent to the cretaceous opening of the south Atlantic ocean. Major horizontal (sinistral) movement along the northeast-southwest axis of the adjacent Benue Trough appear to have been translated to the north-south and north-westering trending shears zones to form the Bida Basin perpendicular to the Benue Trough (Benkhell 1989). Although the sedimentary fill of the Benue Trough consists of three unconformity-bounded depositional successions (Petters, 1978), the Bida and Anambra geographical regions were platforms until the santonian. Pre-santonian marine sediments are recorded principally in the older Benue Trough and part of the southern Anambra Basin. The collapse of the Bida and Anambra platforms led to the sedimentation of the upper cretaceous depositional cycle commencing with the fully marine shales of the campanian Nkporo and Enugu formation which may have some lateral equivalents in the Lokoja formation of the Bida Basin. The detailed stratigrahic description of the succession in the southern and Northern Bida Basin is given below. Greater attention has been given to the Northern Basin from where most of the field data were obtained.

2.1.2 The Batati Formation

This formation constitute the uppermost units in the sedimentary sequence of the Bida Basin. The Batati Formation consists of argillaceous, oolitic and geothitic ironstones with ferruginous clay stone and siltstone intercalations and shaley beds occurring in minor proportions some of which have yield near shore shallow marine to fresh water fauna (Adeleye,1974).

2.1.3 The Enagi Siltstone

The Enagi siltstone consist mainly of siltstone and correlate with the patti formation in the Lokoja sub-Basin other subsidiary lithologies include sandstone siltstone admixture with some clay stone. Fossil leaf impressions and rootlets have been found within the formation. The formation ranges in thickness of between 30m and 60m. Mineral assemblage consists mainly of quartz, feldspar, and clay minerals.

2.1.4 The Sakpe Ironstone

The sakpe ironstone comprises mainly oolitic and pisolitic ironstone with sandy clay stones locally, at the base followed by dominantly oolitic ironstone which exhibits rapid facies changes across the basin, at the top.

2.1.5 The Bida Sandstone

The Bida sandstone is divisible into two members, namely the Doko member and the Jima member. The Doko member is the basal unit and consist mainly of very poorly sorted pebbly arkoses, sub-arkoses and quartzose sandstones. These are thought to have been deposited in a braided alluvial fan setting. The Jima member is dominated by cross-stratified quartzose sandstones, siltstone and clay stones. Trace fossils comprising mainly ophiomorpha burrows have been observed. These were also observed in the overlying sakpe ironstone, suggesting a possible shallow marine subtidal to intertidal influence during sedimentation. The Jima sandstone member is the upper part of the Lokoja sandstone, where similar features also occur.

2.2 Types of Iron ore Deposits

In terms of morphology and mineralogy there are three main types of iron ore that illustrate different ore forming processes including one or more stages during their formation. The three types are banded iron formation (BIF), phanerozoic ironstone, and bog iron (Evans, 1993; Robb, 2004; & Boggs 2006).

2.2.1 Banded Iron Formation

The BIFs represent the most important source of iron ore all over the world, with more reserve and total production value than those of phanerozoic ironstone and bog iron ores. The banded iron formation is a stratigraphic unit composed largely of ironstone that may be cherty or non-cherty but with band appearance (Kimberley, 1989; Klein and Benkes, 1993). BIF are observed over a wide range of scales; from coarse macroband (meters in thickness) to mesoband (centimetre-thick units) to millimetre and sub-millimeter layers (Trendall & Blocklay, 1970). The BIF term is hyphenated and applies strictly to bedded chemical sediment comprising alternating layers rich in iron and chert (Klein & Beukes, 1993). BIF were formed during essentially three periods throughout the Archean and proterozoic Earth history, namely 3500-3000Ma, 2500-2000Ma and 1000-500Ma. The periods equate with different tectonic setting and are referred to as Algoma, Lake Superior and Rapitan types, respectively (James & Trendall, 1982; James, 1983; Maynard, 1991; Klein & Benkes, 1993; Bekker *et al.* 2010, 2014).

2.2.2 Phanerozoic Ironstone

The second type is referred to ironstone deposits formed during the phanerozoic iron deposits. These ironstone deposit are of widespread occurrence representing an important source of iron, particularly during the first part of the twentieth century. The term iron-rich is restricted to sedimentary rocks that contain at least 15% of total iron

(Kimberely, 1994). Iron is present in almost all sedimentary rocks, with average content 4.8% percent in siliciclastic shale 2.4 percent in sandstone and 0.4 percent in limestone (Blatt, 1982). Boggs (2006) used the term ironstone for non-banded, non-cherty, commonly oolitic, iron-rich sedimentary rocks whilst the term iron formation was allocated to the cherty, well-banded iron-rich sedimentary rocks. Several nomenclatures have been used for the phanerozoic ironstone (Bottke, 1981; Barnes, 1989; Evans, 1993; Mucke and Farshad, 2005). Thus, ironstone deposits occurring in the Jurassic sediments of England and the Alase-Lorraine region of France and germany were referred to as minetta or Lorraine-type iron ores other types recorded in North America were known as Silurian Clinton type iron ore of Kentueky and Alabama that are analogues of the younger European deposits (Bottke, 1981; Barnes, 1989; Evans, 1993; Mucke and Farshad, 2005).The ironstone deposit in the phanerozoic were formed in different ways, the most common being the oolite type. This is mainly present in the Ordovician, Silurian, Jurassic, cretaceous and cenozoic periods but shows wide stratigraphic range from percambrian to Holocene (Petranek and Van Houten, 1997). Most oolite ores are economically exploited and major development took place during the Ordovician and Jurassic periods. Ordovician iron oolites are formed in North Africa, Spain, Portugal, france, Poland and other places (James, 1966).

The Ordovician oolite ironstones occur widely in marine shelf sequences of SW Europe (the western European platform) the Avalonian Terrans and in North Africa where they form the most important group of deposits of the two major periods of phanerozoic ooidal ironstone generation (Young & Taylor, 1989). Cenozoic ironstone is also of wide occurrence in the north central Africa and SW Europe in paleocene, Eocene, Oligocene, Miocene and pilocene episodes and mostly with void fabrics 9Van Hutton, 1992). The cenozoic ironstone occurs in northern Pakistan, western Siberia, southern

Germany and central North Africa (Van Hutton, 1992; Petrarek and Van Honter, 1997). The main iron bearing minerals recognized in the phanerozoic ironstone are hematite (Fe_2O_3), goethite (FeO.OH), siderite (Fe CO_3), ankerite (Ca, Mg, Fe)(CO_3), Ferroan dolomite (Ca, Mg, Fe $(CO_3)_2$)Ferroan calcite (Ca, Fe)CO_3), Pyrite (FS_2), Jarosite (KFe_3^{3+} $(SO_4)_2(OH)_6$), chamosite (3(Fe^{2+}, Mg)$_5$Al ($AlSi_3O_{10}$) $(OH)_8$), berthierine (Fe^{2+}, Fe^{3+}, Al, Mg)$_2$.3(Si, Al)$_2O_5(OH)_4$), nontronite (NaO.3Fe_2(Si, Al)$_4$ O_{14}) (OH). nH_2O) and glauconite (K, Mg, (Fe, Al) $(SiO_3)_6$.3H_2O).

2.2.3 Bog Iron Deposits

The third type of iron ore is the bog iron deposits. They mainly form in lakes and swamps of the glaciated tundra regions of the northern hemisphere such as northern Canada and Scandinavia as well as most recent iron deposits (Bogg, 2006). The deposits are typically small and thin and comprise concentrations of goethite and limonite associated with organic rich shale. They formed in recent geological periods; even they form locally at present (Stanton, 1972; Rob, 2004; Boggs, 2006). This type of iron ore precipitates where aqueous solution containing labile ferrons ion (Fe^{2+}), in a relatively reduced environment are oxidized with the subsequent formation and precipitation of ferric iron (Fe^{3+}). The bog iron accumulation occurs at the interface between oxygenated surface waters flowing along an aquifer and the reduced iron-rich solution percolating downwards through a swamp.

2.3 Bida Ironstone

The Bida Ironstone consists of claystone, oolitic ironstone and massive Ironstone, Ladipo *et al*., (1994) proposed the sandstones and claystone to be an over bank depositsand abandoned channel sands. A marine influence occured during the deposition of the Ironstone. Three identifiable facies were recognized by Abimbola (1997): (i) The ooidal pack-ironstone at the base consist of ooids, rich in haematite kaolinite, goethite and kaolinite that formed under high energy shore line encroaching swamp and fluviatile environment (Adeleye, 1973). (ii) Pisoidal pack-ironstone comprises of, loosely packed pisolites and poorly sorted pisolites with goethite, minor haematite and relict kaolinite (iii) at the uppermost part consist of ironstone-mud braccia with a kaolinitic matrix made up of false ooids.

Unlike the relatively simple processes invoked to explain the formation of bog ores, ironstones appear to require a combination of specific environmental conditions, as well as a variety of processes (including oxidation–reduction, diagenesis, mechanical sedimentation, and microbial activity), to form substantial deposits (Imrana & Haruna, (2017).

Siehl & Thein, (1989) proposed that iron initially concentrated on continents were subjected later to a deep weathering and erosion in a humid and warm climatic period. The ooid and lateritic soils were subsequently transferred into a shallow marine environment, either by erosion during regression or flooding during transgression, to be concentrated and reworked in littoral or fluvio-deltaic settings. A discriminate plot of SiO_2 against Al_2O_3 can be used to distinguish between a hydrogeneous ironstone from hydrothermal ironstone (Bonatti, 1975). Chemically precipitated sediment is highly enriched in Fe, Si and Mn while detrital derived ironstone is rich in Al, Zr and Ti.

Onoduku *et al. (*2017), from palynological analysis inferred a non-marine environment of deposition for central Bida sediments which is an indication of terrestrial/fluvial dominated environment and Late Campanian – Early Maastrichtian age was then proposed. The various facies identified by Okosun *et al*. (2007) on the basis of depositional environment within the central Bida basin are: coarse grained channel sandstones and fine medium grained bar top sandstones organized into series of fining upward successions, alluvial fan facies which dominates in the northern part of the basin and consists of channel sandstones and conglomerates, mudstones, sandy mudstones sand silty mudstones , flood plain facies with horizontally laminated fine grained sandstones, mudstones and siltstones and mire facies characterized by lignite/peat beds.

The basal portion of the Bida formation consist of massive erosional based unit, this bodies consist of unit and compound bars that are vertically and extensively stacked showing a sheet like geometry.

Goro *et al*. (2014) proposed two architectural elements mainly an overbank and channel bar. Ojo (2012) proposed a depositional model for the Enagi Formation to be mostly transgressive shallow marine process with frequently incised fluvial channels. A shore face and tidal channel facies of shallow marine environment is suggested. The tidal channel condition occurs due to transgressive channel lag that grades upward. The unidirectional clay stone and cross bedded sandstones indicates floodplains and fluvial channels respectively.

Recent field work by Rahaman *et al.* (2019) in a revise stratigraphy of Bida basin proposed Bida/Lokoja sandstones to be overlay directly by Agbaja/Sakpe Ironstone with the Enagi/Patti formation as the youngest. Their research widely opposed the general views of previous workers that consider Agbaja/Sakpe Ironstone to be the youngest unit in the basin. The Patti formation was redefining as Ahoko formation based on stratigraphic principles, since the sequence of rock used to define Patti formation was absent in mouth Patti but present at Ahoko village.

2.4 Origin of Ironstone in Bida Basin

The Bida ironstone was initially proposed to be of the European Minnete-type deposits by Jones (1965) but was later opposed by Mucke et.*al.* (1999) due to low concentration of magnesium oxide and abundance of kaolinite, as the primary matrix and thereby proposed a kaolinite type deposit. A pre-requisite for the formation of chemosite such as predominance of reducing condition and availability of magnesium were lacking. Kogbe (1978) indicates that Bida ironstone is similar to that of Sokoto basin and lateritic origin was propose but his work failed to explain the presence of the kaolinite ooid that is present in the Bida ironstones. Adeleye (1973) suggested a deposition in a deltaic – lagoonal environment, primarily derived from metamorphic and igneous protholith. The oxide and trace element relationship plotted on discriminant plot by Hasan *et al*. (2019) shows a diagenetic origin with a detrital source and dispose the idea of possible marine source.

2.5 Tectonic History of Bida Basin

The inland basins of Nigeria constitute one set of a series of Cretaceous and later rift basin in Central and West Africa whose origin is related to the opening of the South Atlantic. The upper Cretaceous Bida Basin of central Nigeria is sandwiched between the Precambrian schist belt of the Northern Nigeria massif and the West African craton. Of interest is the southern part of the basin, which developed in a continental setting, because the facies architecture of the sedimentary fill suggest a close relation between sedimentation dynamic and basin margin tectonics (Sokar, 1990). This relationship is significant to an understanding of the basin origin, which has been controversial. A simple sag and rift origin has been suggested and consequently dominated the negative thinking on the hydrocarbon prospects of the basins, which were considered poor. Although distinguishing pull-apart basins from rift basins, based solely on sedimentary logical grounds, may be difficult, the temporal migration of the depocenter, as well as the basin architecture of repeatedly upward-coarsening, show a strong tectonic and structural overprint that suggests a tectonic framework for the southern Bida basin similar in origin to a pull-apart basin which was based solely on the sedimentological evidence proved to be a difficult mechanism (Sokar, 1990).

The Bida basin is a gently down-warped trough whose genesis maybe closely connected with the Santonian oroganic movements of south eastern Nigeria. The basin is a NW-SE trending embayment, perpendicular to the main axis of the Benue Trough and Niger Delta Basin. It is frequently regarded as the north-western extension of the Anambra Basin, both of which were major depocentres during the third major Transgressive cycle of southern Nigeria in Late Cretaceous. Interpretations of LandSat images, boreholes logs, as well as geophysical data across the entire Bida Basin suggest that the basin is bounded by a system of linear fault trending NW-SE. Gravity study also confirm central positive anomalies flanked by negative anomalies as shown from the adjacent Benue Trough and typical of rift structure (Ojo, 1984; Ojo & Ajakaiye, 1989). The Benue Trough is a failed arm of a triple junction (aulacogen) that existed beneath the present position of the Niger Delta during the Cretaceous. The trough is filled with over 5000m of predominantly Aptian to Maastrichtain sediments in the lower, middle and upper Benue geographical regions. The Lower Benue Trough which includes the Anambra Basin is considered as the southern extension of the Bida Basin. Initial gravity studies in the Bida Basin put the maximum thickness of the sedimentary succession at about 3.5km (Ojo, 1984) in the central axis. Although the hydrocarbon potential of the basin has not been fully tested; the basin remains undrilled. Both ground and aeromagnetic studies by several workers have outlined the basin's configuration (Adeniyi, 1985; Udensi and Osazuwa, 2004). A recent spectral 99 analysis of the residual total magnetic field values over several sections of the basin reveals an average depth to the basement rock to be approximately 3.4km with sedimentary thickness of up to 4.7km in the central and southern parts of the basin (Udensi and Osazuwa, 2004). In general, sediment thickness decreases smoothly from the central portion to the flanks of the basin as shown in Figure 3.

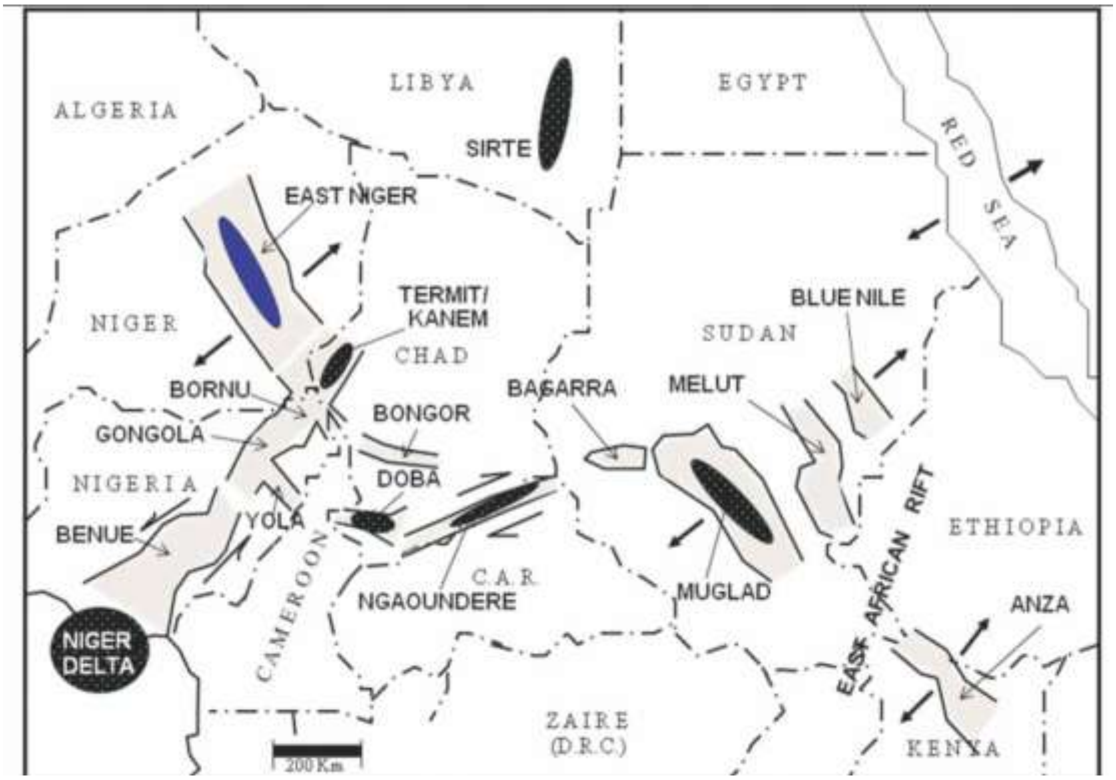

Figure 3: Regional tectonic map of western and central African rifted basins showing the relationship of the Muglad, Doba and East Niger Basin to Nigeria inland basins. Location of regional shear zones (marked with half-arrow) and major zones extension (complete arrow) are shown. (Schull, 1988)

CHAPTER THREE

3.0 MATERIALS AND METHODS

3.1 Material used

The main material used for the study is an ironstone sample collected from an exposed outcrop.

Plate I: Ironstone sample (DOKO)

3.2 Methods

3.2.1 Fieldwork

The main aim of the fieldwork exercise was to collect representative samples of the rock (ironstone) in the following project areas; Doko, Bida-Lemu Road and Kutigi and to study the geology of the area. The samples comprised of ironstone which were collected by grabbing. The samples were labelled using the following convention, the first two letters of the sample numbers is an indication of my name and location for example JD for Joshua Doko, JBL for Joshua Bida-Lemu Road and JK for Joshua Kutigi. The number indicates the sequence in which they were collected. The methodology employed during the fieldwork exercise could be summarised as follows:

i. Study of the ironstone database with emphasis on lithology and structures
ii. Collection of representative fresh samples from each lithology present in the different location.
iii. Description of the ironstone and collection of samples by grabbing
iv. Photography of all samples outcrop and structures
v. Search for literature on ironstone form Bida-Basin.

3.3 Laboratory Studies

3.3.1 X-Ray Fluoresce (XRF) Analysis

The samples were pulverized using aplanetary micro mill (pulverisette 7) to pass 150 micron mesh sieves. About 5g of the pulverized sample was weighed into a beaker with the addition of 1g of starch binder. The thoroughly mixed material was pressed under high pressure (6 tonnes) to produce pellets. Approximately 0.4g of sample was fused with 7.6g flux to produce glass beads. The samples were analysed for major and trace element concentration using an Energy Dispersive X-ray fluorescence (EDXRF) spectrometer (model "Minipal 4"). Loss on ignition (LOI) was determined gravimetrically by heating 1g of the powdered sample at 1000^oC

3.3.2 X-Ray Diffraction (XRD) Analysis

The sample powders (< 150 microns) were smeared evenly on the sample holder made of aluminium material and analysed using a Schimadzu Model 6000 X-ray diffraction spectrometer. The analyses were carried out between 2 to 60 degrees 2θ as the sample scanning range and the scanning rate was set at 6 degree per minute.

3.3.3 Beneficiation

Materials required: High intensity magnetic separator, Bida Iron ore, electronic weighing machine, collection pans, jaw crusher, Ball mill.

3.3.3.1 Method of Beneficiation

The concentration of Bida Iron ore by magnetic concentration method was carried out according to the following steps;

i. The ore was pulverized to about 100 percent passing 125um.

ii. The electro-magnetic separator was induced by allowing current to pass through it.

iii. 200g out of the ground sample was introduced into the device (electro-magnetic separator) and the setting was maintained at the selected voltage.

iv. The process was allowed to run for ten (10) minute to ensure that the efficient separation was achieved.

v. After ten (10) minutes, the products were collected and weighed.

3.3.4 Sample Preparation for X-Ray fluoresce (XRF) Analysis

This technique is chosen because it is a non-destructive analytical technique used to identify and determine the concentration of elements present in solid, powered and liquid samples. XRF is capable of measuring elements from Beryllium (Be) to Uranium (U) at trace levels and up to 100%. It is the most widely used analytical technique in the determination of the major and trace elements chemistry if rock samples (Rollinson, 1993). It is based on the formation of fluorescence as result of the quantum energy released when an atom is de-excited after irradiation with x-rays. The x-ray photons are a form of electromagnetic radiation (10-100ev range of energy). They are produced when high speed electrons decelerate or when electron transition occur involving inner orbit energy state of atoms. When any sample is bombarded with electron radiation (irradiation), an inner shell electron is ejected, which leaves the atom in an excited state. A de-exictetion process occurs to return it to a stable ground state. The vacancy created by the emission of an inner shell electron is filled by an electron previously residing at a higher energy level. The excess energy resulting from the transition of often dissipated as electromagnetic radiation called x-ray photon. These photons have a narrow energy bandwidth and are specific for particular electro transition that occurred and are characteristic of the elements from which they are emitted. The x-ray that is emitted by the sample are absorbed by the detector which act as chiode in converting these incident x-ray to electronic pulres whose amplitude are proportional to the energies of the corresponding x-rays. The pulses are processed and sorted according to the amplitude. The entire range of pulses amplitude is divided into 1024 intervals called channels and those pulses filling within each interval are counted in a multi-channel analyzer. The channel member is usually converted into units by calibrations. The intensity or member of counts in a peak is a direct result of the member of fluorescing atoms of that element in the sample. Thus, the area under a peak is proportional to the concentration of that element in the sample.

CHAPTER FOUR

4.0 RESULTS AND DISCUSSIONS

4.1 Field Aspect

Field outcrop description was carried out by careful observation of the lithology of ironstone. The ironstone deposit is mainly of the sedimentary type. The basal beds are conformably over-lain by a lithology comprising mainly sandstones and subsidiary claystone, fine conglomerates and siltstones. Massive appearance and flat beds are most common in the basal area of the sandstones, while the upper shows widely developed large scale cross stratification.

Plate II: Photograph of ironstone bed at 8^0 56' 43.3''N, 5^0 57'26.2''E (DOKO)

4.2 Field Outcrop Description

4.2.1 Thin Ironstone Bed

This ironstone at Bida-Lemu Road is situated at the north-western part of the study area and account for 70% of the study area. Ironstone type is brownish in colour. A thin ironstone bed underlay by ferruginous sandstone bed and overly by friable sandstone bed.

Plate III: Photograph of ironstone bed underlying ferruginous sandstone at 8°56'43.3" N, 5°57'26.2"E (Bida-Lemu Road)

4.2.2 Cross-section of Horizontal Bed

This cross-section of horizontal bed is located at Bida-Lemu Road in the north-western part of the study area and account for 40% of the study area. The cross-section of the horizontal beds of sandstones, siltstone and capped ironstone at the top.

Plate IV: Photograph of cross-section of horizontal beds at 9° 9' 49.1"N, 6° 61' 24.2"E (Bida-Lemu Road).

4.2.3 Concretion Ironstone

This ironstone is located at Kutigi north-eastern part of the study area and account for about 20% of the study area. The ironstone is dark-brown in colour. The concretional ironstone is interbedded within a sandstone bed.

Plate V: Photograph of concretion ironstone at 09° 12' 2.3"N, 05º 35' 22.3"E (Kutigi)

4.2.4 Horizontal Bed of Siltstone

This ironstone is located at Bida-Lemu Road which is the north-eastern part of the study area and account for about 10% of the study area. The ironstone is dark-brown in colour and hhorizontal bed of siltstone with bioturbated sandstone at the top.

Plate VI: Siltstone with bioturbated sandstone at 09° 12' 02.3"N, 05° 35' 23.2"E (Bida-Lemu Road)

4.3 Mineralogy

The results of X-ray diffraction analysis are presented in Table 4.1 and representative diffraction patterns are presented at Figure 4.9.1. Three minerals, namely hematite, magnetite and quartz were identified in sample JD1. Hematite is the dominant mineral within the sample, accounting for up to 70%, followed by quartz at 25% and magnetite at 5%. For sample JBL3 hematite is the dominant mineral in the sample, accounting for 71%, quartz at 21% and magnetite at 8%. In sample JK1 Hematite account for 68%, with quartz at 25% and magnetite 7%.

Table 4.1 Mineral abundance in percentage for ironstone in Bida Basin for location JD3 Mineral Abundance (%) of Ironstone for Bida Basin for location JD3

Minerals	Percentage %
Quartz	25
Hematite	70
Magnetite	5

Table 4.2 Mineral abundance in percentage for ironstone in Bida Basin for location JBL3Mineral Abundance (%) of Ironstone for Bida Basin for location JBL3

Minerals	Percentage %
Quartz	21
Hematite	71
Magnetite	8

Table 4.3 Mineral abundance in percentage for ironstone in Bida Basin for location JK1 Mineral Abundance of Ironstone for Bida Basin for location JK1

Minerals	Percentage %
Quartz	25
Hematite	68
Magnetite	7

4.4 Discussion of Mineralogy Result

The results of X-ray diffraction analysis are presented in Table 4.1, 4.2 and 4.3 and representative diffraction patterns are presented in Figure 4.1, 4.2 and 4.3.Three minerals, namely Hematite, Magnetite and quartz were identified in sample JD3, JBL1 and JK1.

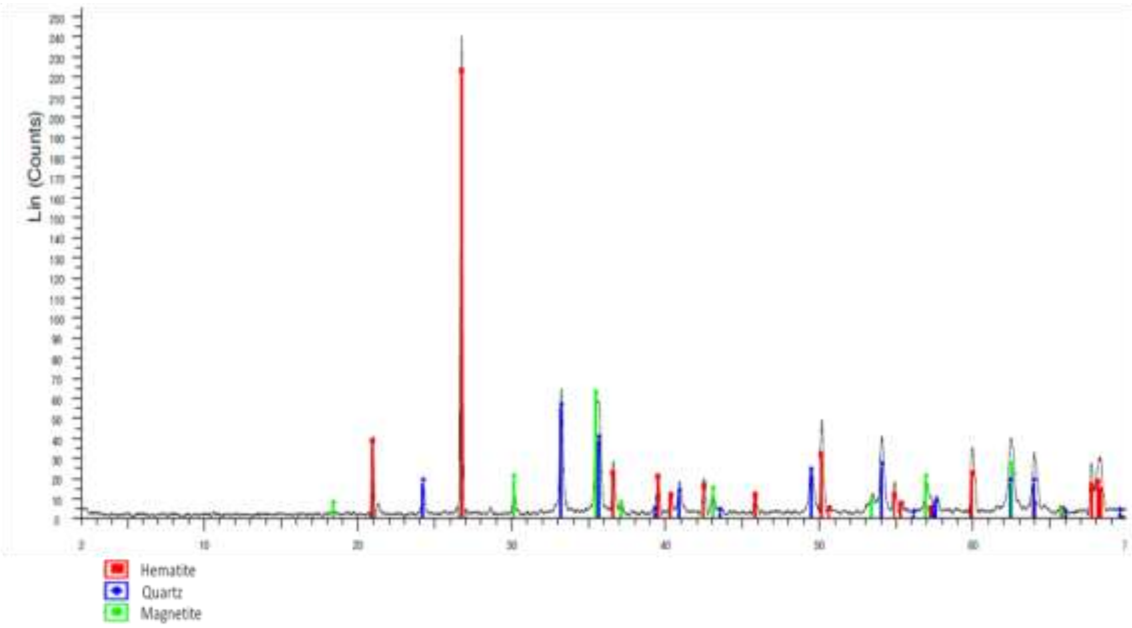

Figure 4.1: XRD diffraction for sample JD3 showing Hematite as the main Fe oxide

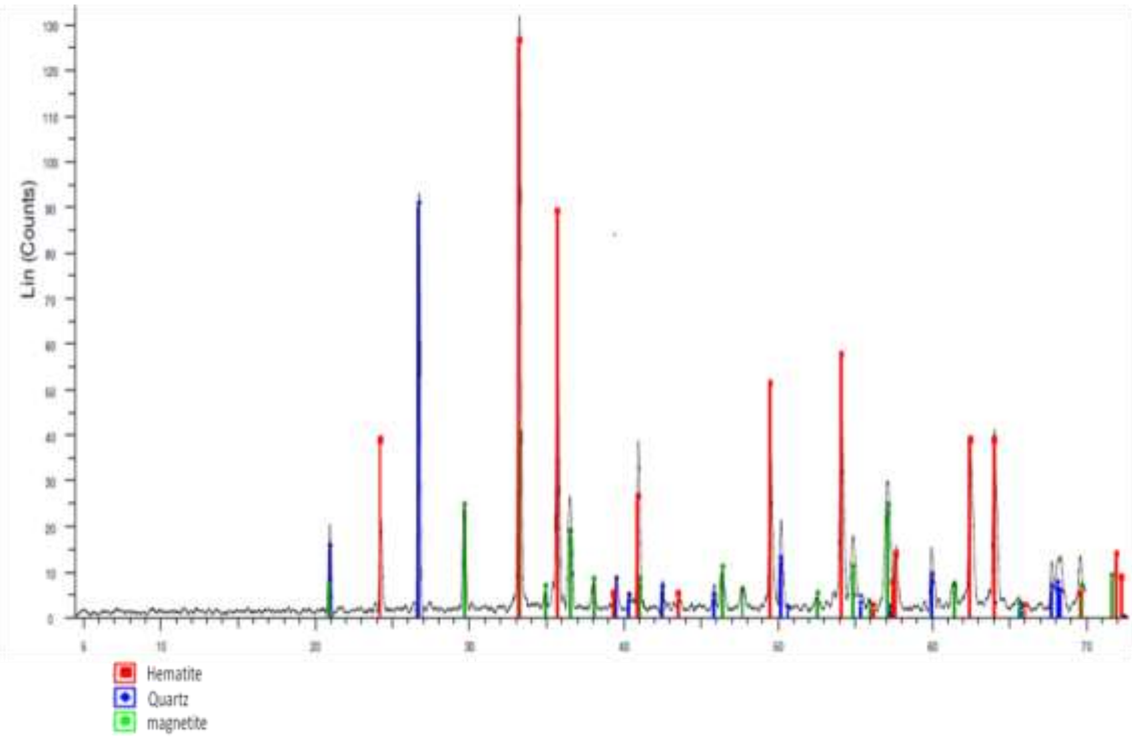

Figure 4.2: XRD diffraction for sample JBL3 showing Hematite as the main Fe oxide

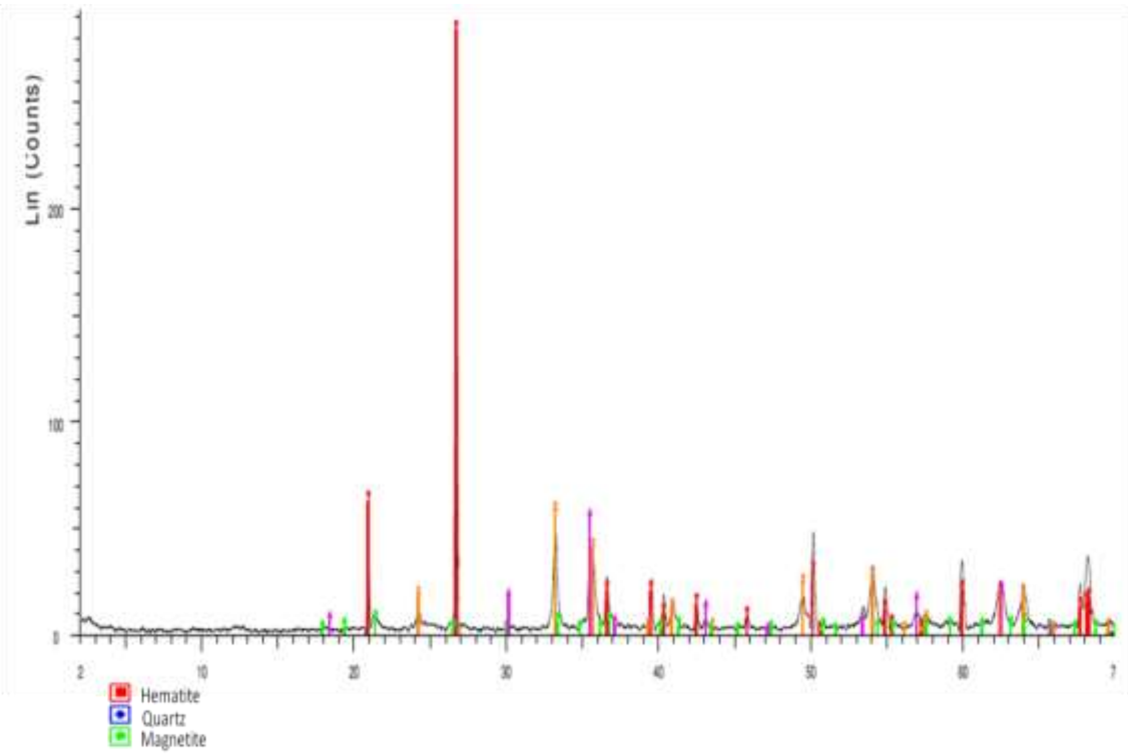

Figure 4.3: XRD diffraction for sample JK1 showing Hematite as the main Fe oxide

4.5 Result Interpretation

4. 6 Geochemistry

Table 4.6.1: Major elements compositions of Ironstone from the study area (values in wt %)

Samples/ Oxides	**JD1**	**JD2**	**JD3**	**JD4**	**JBL1**	**JBL2**	**JBL3**	**JBL4**	**JK1**	**JK2**	**JK3**	**JK4**
SiO_2	24.1	22.66	20.43	24.02	21.03	24.88	27.06	27.98	28.04	24.08	25.01	26.38
Al_2O_3	3.22	4.76	1.78	3.02	1.66	1.67	2.33	2.43	0.98	1.78	2.06	1.22
Fe_2O_3	66.88	65.43	70.02	67.11	66.7	64.5	59.99	59.11	60.13	63.66	63.87	61.22
CaO	0.06	0.08	0.04	0.12	0.22	0.01	0.07	0.13	0.11	0.07	0.04	ND
Na_2O	0.05	0.03	0.06	0.01	0.09	0.1	0.21	0.11	0.06	ND	ND	0.15
K_2O	0.022	0.018	0.017	0.008	0.013	0.023	0.001	0.018	0.023	0.004	0.066	0.013
TiO_2	0.45	0.55	0.01	0.66	0.11	0.23	ND	0.44	0.05	0.21	0.33	ND
MnO	1.09	0.99	0.34	ND	0.44	0.32	0.33	ND	ND	1.02	1.04	0.36
TOTAL	**95.87**	**94.52**	**92.69**	**94.95**	**90.26**	**91.73**	**90.12**	**90.22**	**89.43**	**90.78**	**92.96**	**89.34**

4.7 Major Element Composition

The major rock types underlying the study area comprise of sandstone siltstone and ironstone rocks. The major elements analysis shows that the ironstones are characterized by low SiO_2in the range of 21.03 – 28.04wt % with an average of 24.64wt%. High content of Fe_2O_3 (59.11- 66.88wt %), Alumina (Al_2O_3) contents for all the ironstone types are generally within the range of (0.98-4.76 wt%). This values falls within the average continental contents of these rocks. Also, the rocks have aluminum saturation index [defined as the molar ratio of Al2O3/ (CaO+Na2O+K2O) after Ekwume (2003) greater than one (1) and consequently falls within the corundum norm except for the hornfel with Al_2O_3(CaO+Na2O+K2O) < 1 probably due to high content of CaO even greater than Al_2O_3, hence cannot have corundum in it norm.

4.7.1 Origin of the Ironstone

The ironstone in this study is located in a sedimentary terrain of Bida Basin that is composed of rocks. The ironstone in the study area is similar to that of Konton-Karfe in terms of texture; both are fine-grained with similar mineralogical compositions of magnetite, quartz and other accessory minerals. The Al_2O_3- concentration (4.76 wt% on average) of the ironstone in the study area is comparable to the range of values of Al_2O_3-concentration of other ironstone values at Unguwar - Malam Ayuba (ranging from 2.3 to 18.5 wt %) as revealed by Mucke (1994).

The high Al-content in the Nigerian iron-formations is probably as a result of the continuous supply of continental material into the marine basin. Therefore, it can be deduced that the SiO_2- content of the iron-formation is not necessarily from the exhalative origin only but may also be of continental origin.

This ironstone therefore could be taken to belong to the magnetite-silicate facies type that has been exhaustively studied by several workers such as Ibrahim (2002); Adekoya, (1996) and Mucke *et al*. (1996) in 64 many NW, central and SW Nigeria occurrences. Terrigeneous source is envisaged to have provided the material for the ironstone.

It is now widely believed that the materials for the formation of ironstone globally are derived from two main sources: continental granitic rocks and volcano-sedimentary deposits (Khan *et al.,* 1996; Adekoya, 1996; Mucke *et al*., 1996 and Ibrahim, 2002). A ternary plot of Fe-Mn-(Cu+Zn)*10 is plotted for the ironstone in the study area. The Figure 4.3 shows that the ironstone is from submarine-hydrothermal source.

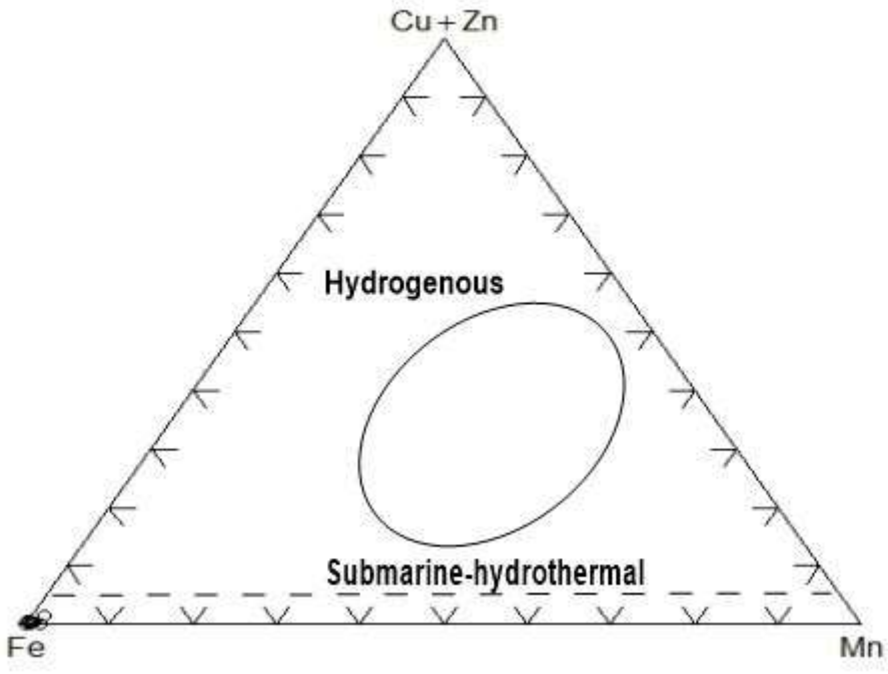

Figure 4.4: Fe-Mn-(Cu+Zn) diagram to differentiate submarine hydrothermal and hydrogenous deposit (Bonatti *et al*., 1972) and the analytical plot of the ironstone in the study area.

Based on figure 4.7.2.2 below, the ironstone in the study area falls within the field of magnetite-silicate facies and lies close to the (FeO+MnO)-SiO_2 join**.** Therefore, the ironstone in the study area is of the magnetite-siliciate facie type. It is not the most wide spread type of iron formation in Nigeria that is developed in all the schist belt of northern Nigeria especially in the Malumfashi in (Tudun Kudu and Unguwar Malam Ayuba areas), Birnin-Gwari schist belts and in Isanlu in Central Nigeria (Mucke *et al*., 1994) and that of Kazaure schist belt (Danbatta, 1999; Ibrahim, 2002).

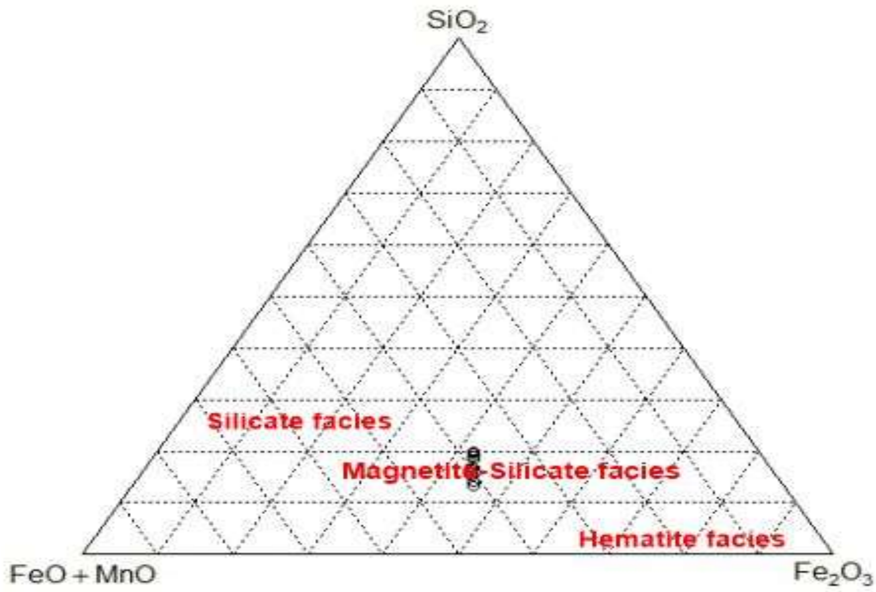

Figure 4.5: A ternary plot of SiO2; FeO + MnO; Fe2O3, (After Mucke, 2005). The ironstone in the study area all fall within the magnetite-silicate facie type

4.8 Regression Analysis and Fitted Line

This is an analysis that generates an equation to describe the statistical relationship between one or more predictors and the response variable; and to predict new observations. Regression generally uses the ordinary least squares method which derives the equation by minimizing the sum of the squared residuals. Regression results indicate the direction, size, and statistical significance of the relationship between a predictor and response. Sign of each coefficient indicates the direction of the relationship. Coefficients represent the mean change in the response for one unit of change in the predictor while holding other predictors in the model constant. The equation predicts new observations given specified predictor values. The Fitted line plot is also used to investigate the relationship between two continuous variables: a response and a predictor. When a fitted line plot is created, the response variable is displayed on the y-axis and the predictor variable on the x-axis, and then the regression model (linear, quadratic, or cubic) that best describes the relationship between them is chosen. This statistical analysis was carried out using (Microsoft Excel) to predict the type of relationship that exist between the main elemental oxide of interest that is Fe_2O_3 and the other elemental oxide (such as SiO_2, Al_2 O_3,CaO, MgO, P $_2$O $_5$, SO_3, TiO_2 and MnO) which exist in considerable amounts. From the result of the regression analysis, it was observed that SiO_2 and Al_2O_3 have inverse relationship with a degree of variation response of 64.9% and 48.9% respectively. PO_5 has a direct relationship with the Fe_2O_3 with 65.7% variation response. Whereas SO_3, TiO_2, MnO and CaO also have a direct relationship with the Fe_2O_3 but with low level of variation responses of 3.0%, 20.8%, 12.7% and 11.5% respectively. MgO from the sample does not have any relationship with theFe_2O as shown by the fitted line plot and the response of 0%. As observed by it is difficult and sometimes controversial to explain the origin of ironstones geochemically, because of complexities in the processes of iron (Fe) concentration in supergene environment and formation of ironstone associated with theories .However, it suggest that the positioning of the various elements given in Goldschmidt's classification (lithophile, siderophile, chalchophile and atmophile) in the periodic table can form the basis for the relationship between the elements and iron. Silicon a non metallic lithophile element has an inverse relationship with the metallic siderophile iron because of the greater electron affinity that exists between them. Aluminum a metalloid and a lithophile element have an inverse relationship with iron a siderophile element.

Phosphorus a poly atomic non metallic siderophile element has the affinity to a liquid metallic phase, and its response value is the highest which signifies that it shares some common chemical characteristic with the iron. Calcium, a lithophile and an alkaline earth metal has a low electron affinity to iron hence, the response is low but they do share certain common metallic properties. sulphur is a poly atomic non metallic chalcophile that has a high electron affinity to metals. Titanium and Manganese are lithophile elements and have a direct relationship with iron a siderophile element because all of them are from the transition block and same period in the periodic table; therefore they share certain chemical properties. Magnesium a lithophile element that is almost absent in the Banded Iron Formation (BIF) but due to the nature of the sedimentary iron ore, some traces are found thereby, the response is 0 %.

S = An estimate of standard deviation of the error in the model.

R2 (R-sq) = Coefficient of determination; indicates how much variation in the response is explained by the model. The higher the R2 the better the model fits your data.

Adjusted R2(R Adj) = Accounts for the number of predictors in your model and is useful for comparing models with different numbers of predictors.

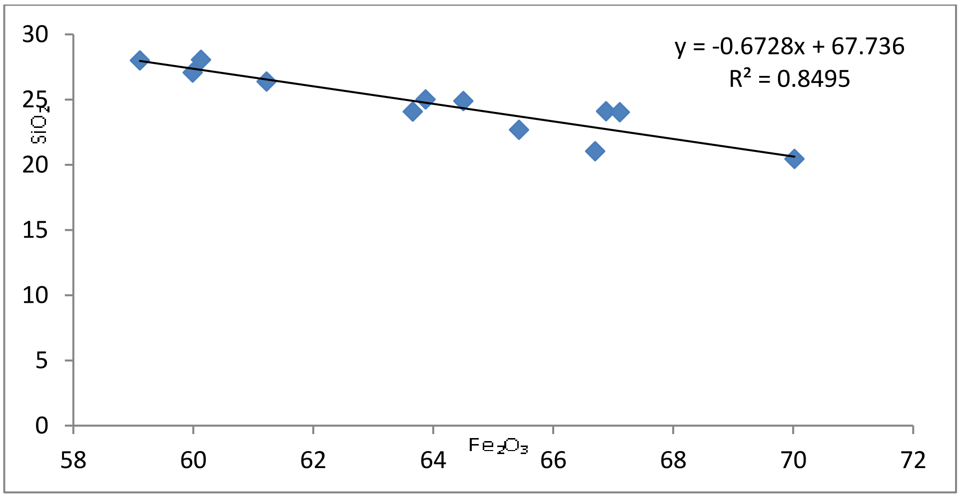

Figure 4.6(a) Regression Analysis with Fitted Line: SiO2 versus Fe2O3

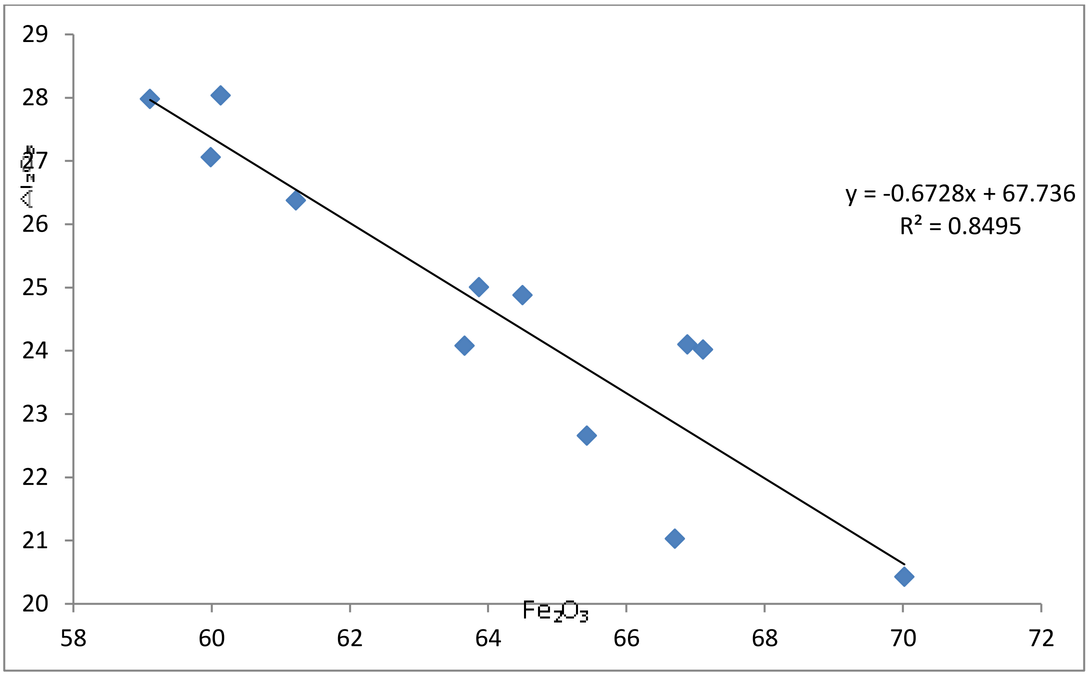

Figure 4.61(b) Regression Analysis with Fitted Line: Al_2O_3 versus Fe2O3

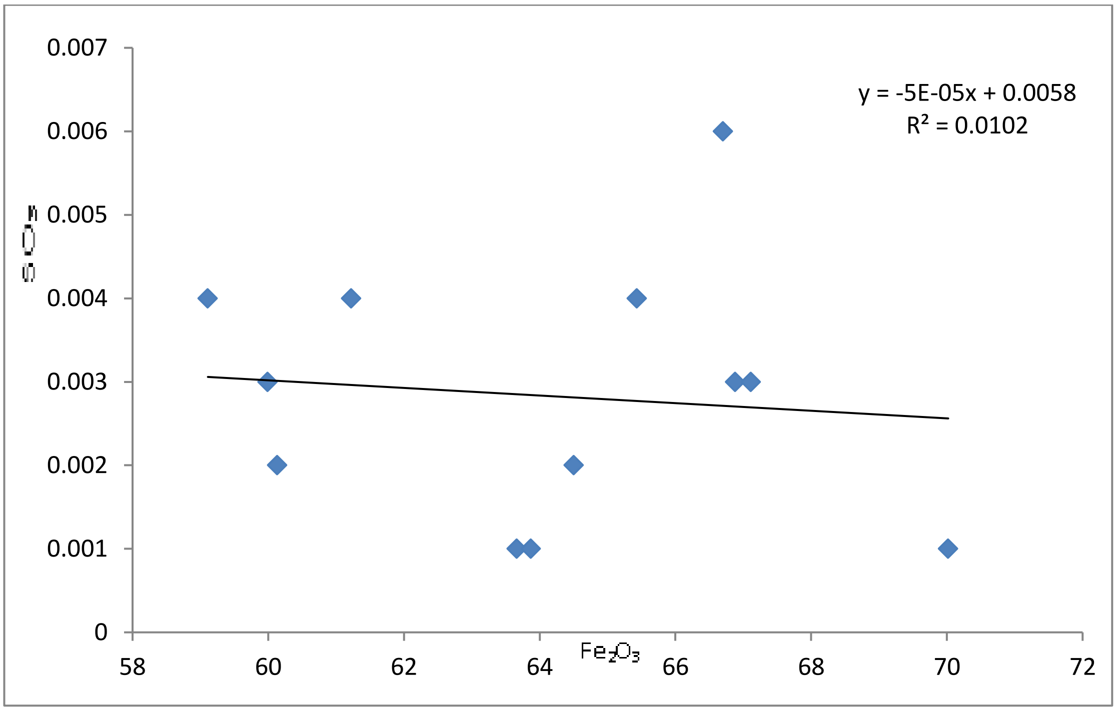

Figure 4.6(c) Regression Analysis with Fitted Line: SO_3 versus Fe_2O_3

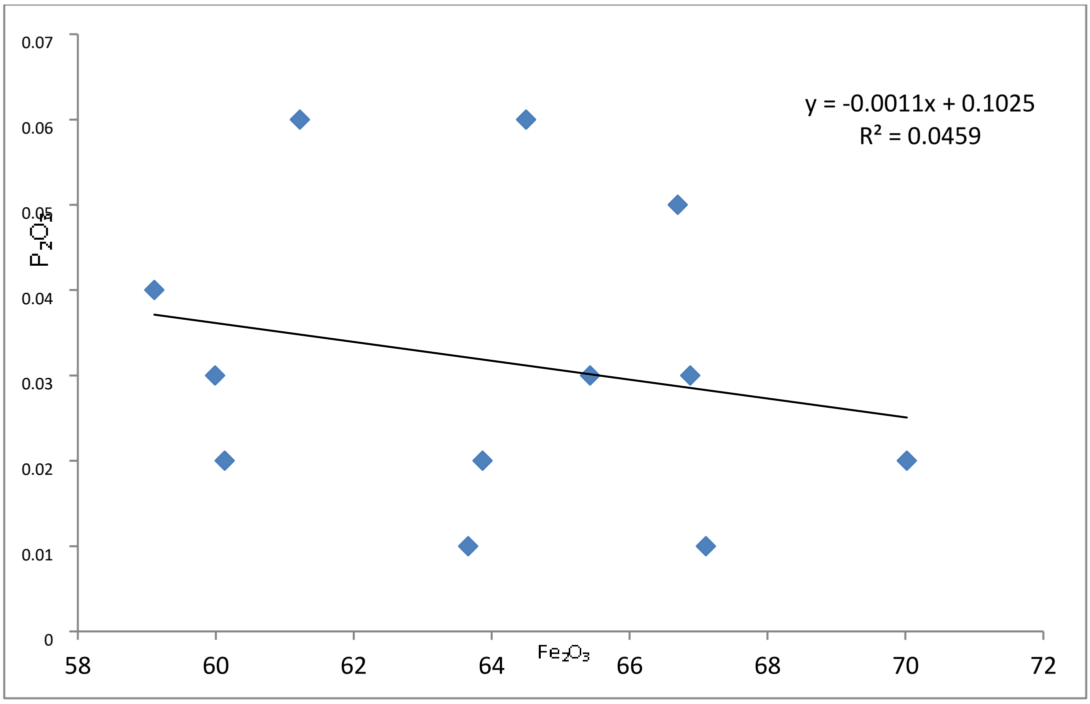

Figure 4.6(d) Regression Analysis with Fitted Line: P_2O_3 versus Fe_2O_3

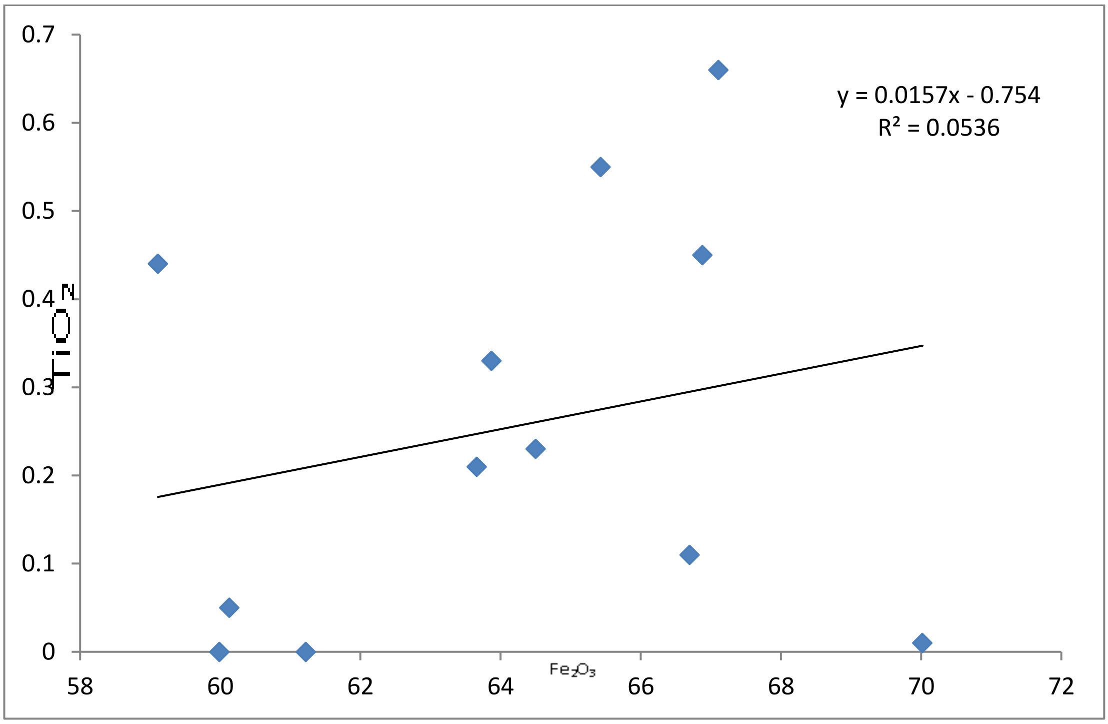

Figure 4.6(e) Regression Analysis with Fitted Line: TiO_2 versus Fe_2O_3

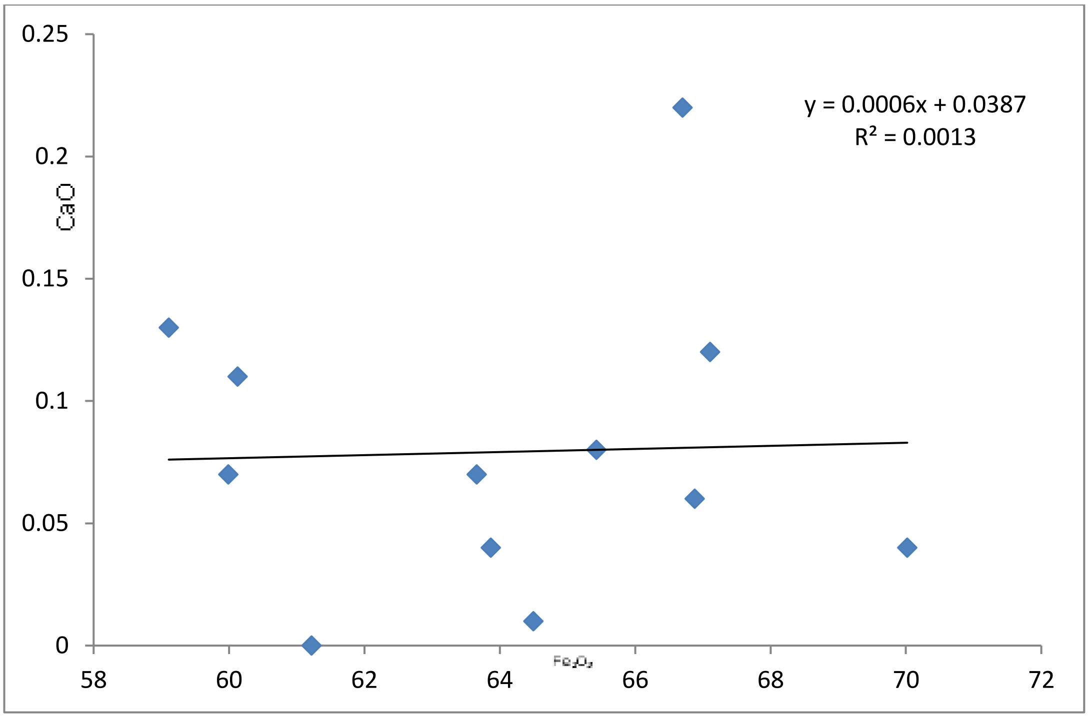

Figure 4.6(g) Regression Analysis with Fitted Line: CaO versus Fe_2O_3

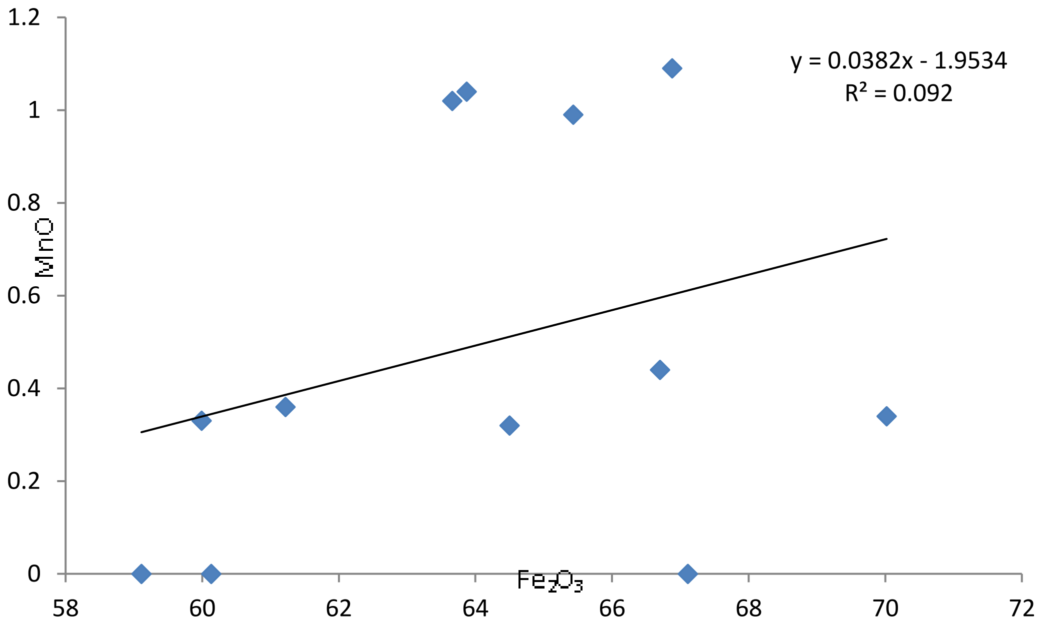

Figure 4.6(g) Regression Analysis with Fitted Line: MnO versus Fe_2O_3

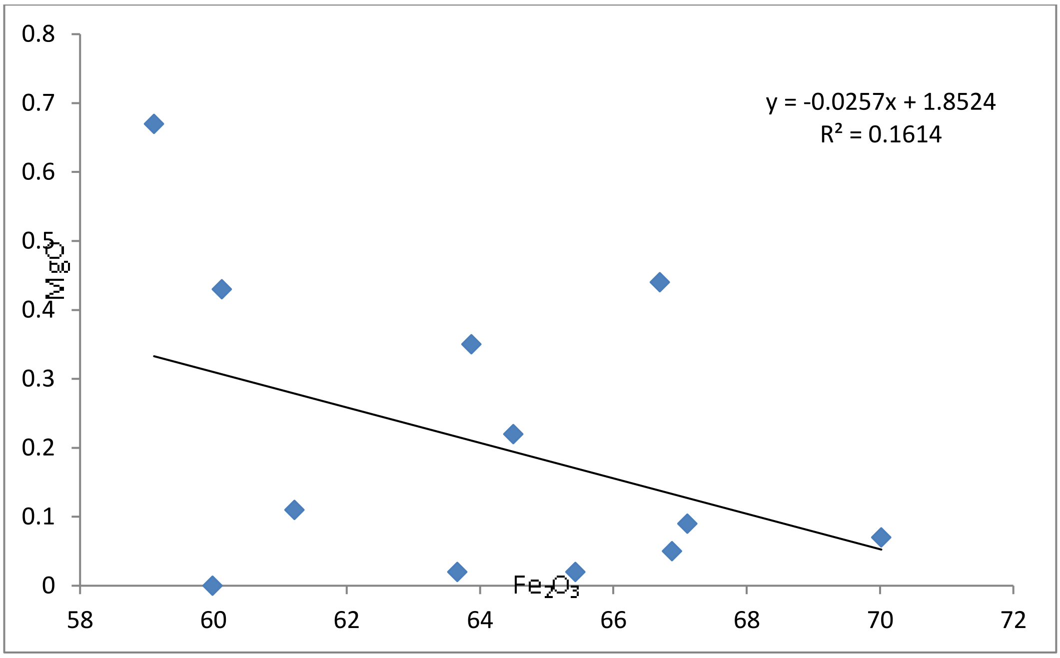

Figure 4.6(h) Regression Analysis with Fitted Line: MgO versus Fe_2O_3

4.8.1 Grade of determination

Table: 4.8.1: Generalized Percentages of Element of Major interest in Assessing Iron ore quality

Components	Total Fe			SiO_2	Al_2O_3	Phosphorous	Sulphur
Content (Mass %)	Low (L) <58	Medium (M) 62-64	High (H) >65	<6	3-4	0.05-0.07	0.1

To understand and assess the quality and grade of Bida Basin ironstone, the contents of the major elements in this ore was compared with the composition of extracted ores from other nations. Among the biggest iron ore producing nations are China, Brazil, Australia, India, Russia, and the USA. To determine the grade, the iron oxide (Fe_2O_3) has to be converted to elemental state of iron (Fe total). To achieve this, value of the oxide content is multiplied by its conversion factor. From the result of Bida Basin ironstone in Table 4.4.1 Fe_2O_3 content ranges from 59.11% to 66.88% with an average of 64.05%. The conversion is explained below.

Fe wt=55.847g

O wt =15.999g

Molecular weight of Fe_2O_3 =2(55.847) + 3 (15.999)=159.69g/mol

For the iron (Fe total) proportion = Fe2/ Fe2O3=2(55.847l/159.69= 111.694159.69⁄=0.6994

Therefore, the average of Fe2O3 (67.81%) when multiply by the conversion factor the average percentage grade of Fe

For example; grade of Fe= 64.05×0.6994= 44.79% (Grade)

From this calculation, Bida Basin ironstone is of low grade using the generalized percentages of element of major interest (Dobbins and Burnet 1982) in assessing its iron ore quality.SiO2 content between 21.08% -28.04% in Bida Basin is higher than the generalized percentage of < 6 %. Based on the analysis of SiO_2contents, it may be concluded that the iron ores from Bida Basin deposit cannotserve well as a good raw material for steel production but rather good for cast iron production. The major effect of silicon is to promote the formation of grey iron. Grey iron is less brittle and easier to finish than white iron. It is preferred for casting purposes for this reason.

Turner reported that silicon also reduces shrinkage and the formation of blowholes, thus lowering the number of bad castings. Phosphorus makes steel brittle, even at concentrations of as little as 0.6%. Bog ore often has high phosphorus content. The strength and hardness of iron increases with the concentration of phosphorus as low as 0.05% phosphorus in wrought iron makes it as hard as medium carbon steel. Phosphorous content of Bida Basin iron stone on an average from this study is 0.03% which is lower than the recommended valve of 0.05–0.07%. Aluminium oxide increases the viscosity of the slag. High aluminium will also make it more difficult to tap off the liquid slag during production. Aluminium in Bida Basin iron ore from this study ranges from 0.98%- 4.76% with an average of 2.24%. This is lower than the permissible level of 3-4% set for direct iron production without prior beneficiation. In Bida Basin iron ore, sulfur content ranges from 0.001% -0.006% with an average of 0.003 which seem to be metallurgical low and unacceptable for high quality iron and steel production.

Sulfur dissolves readily in both liquid and solid iron at the temperatures present in iron smelting. The effects of even small amounts of sulfur are immediate and serious. Small cracks on hot iron can cause the object to fail during use. The degree of failure is in direct proportion to the amount of sulfur present. According to, good foundry iron should have less than 0.15%sulfur.

4.9 Geochemistry

The result of the X-ray fluoresce (XRF) analysis is presented in the table below;

Table 4.9.1: X-ray Fluoresce (XRF) analysis

Wt. % Oxides	JD1	JD2	JD3	JD4	JBL1	JBL2	JBL3	JBL4	JK1	JK2	JK3	JK4
SiO_2	24.1	22.66	20.43	24.02	21.03	24.88	27.06	27.98	28.04	24.08	25.01	26.38
Al_2O_3	3.22	4.76	1.78	3.02	1.66	1.67	2.33	2.43	0.98	1.78	2.06	1.22
Fe_2O_3	66.88	65.43	70.02	67.11	66.7	64.5	59.99	59.11	60.13	63.66	63.87	61.22
TiO_2	0.45	0.55	0.01	0.66	0.11	0.23	ND	0.44	0.05	0.21	0.33	ND
MgO	0.05	0.02	0.07	0.09	0.44	0.22	ND	0.67	0.43	0.02	0.35	0.11
Na_2O	0.05	0.03	0.06	0.01	0.09	0.1	0.21	0.11	0.06	ND	ND	0.15
CaO	0.06	0.08	0.04	0.12	0.22	0.01	0.07	0.13	0.11	0.07	0.04	ND
K_2O	0.022	0.018	0.017	0.008	0.013	0.023	0.001	0.018	0.023	0.004	0.066	0.013
MnO	1.09	0.99	0.34	ND	0.44	0.32	0.33	ND	ND	1.02	1.04	0.36
P_2O_5	0.03	0.03	0.02	0.01	0.05	0.06	0.03	0.04	0.02	0.01	0.02	0.06
SO_3	0.003	0.004	0.001	0.003	0.006	0.002	0.003	0.004	0.002	0.001	0.001	0.004
Fe_3O_4	4.77	5.99	5.33	4.33	3.99	4.90	4.54	4.90	5.67	5.90	3.90	5.44
V_2O_5	0.008	0.09	0.05	0.13	0.004	0.055	0.006	0.001	0.002	0.004	0.03	0.044
Cr_2O_3	0.055	0.011	0.066	0.043	0.022	0.034	0.004	0.033	0.032	0.011	0.087	0.067
SrO	0.44	0.54	0.5	0.23	2.01	2.00	0.77	0.34	0.55	0.44	0.30	0.31
ZnO	0.022	0.032	0.011	0.23	0.221	0.044	0.036	0.022	0.23	0.073	0.033	0.087
BaO	0.11	0.54	0.44	0.23	0.12	0.66	0.86	0.23	0.44	0.33	0.21	0.11
CuO	0.012	0.045	0.003	0.048	0.021	0.055	0.12	0.044	0.096	0.055	0.033	0,073
LOI	1.22	1.11	2.90	2.11	1.22	1.71	3.01	2.76	1.90	2.34	1.90	3.11
	102.592	102.39	101.648	102.402	98.367	101.473	99.37	99.262	98.765	100.008	99.28	98.685

The concentration of Fe_2O_3 range from 59.11 - 66.88wt% with an average of 64.05wt% and SiO_2 range from 21.03-28.0wt% with an average of 24.64wt%. The concentration of P_2O_5, k_2O and CaO range from 0.01-0.06wt%, 0.001-0.066wt% and 0.01-0.22wt% with average values of 0.03wt%, 0.02wt% and 0.085wt% respectively. TiO_2 ranges from 0.01-0.66wt% with an average of 0.3wt%, Na_2O, MgO and Al_2O_3 ranges from 0.1-0.09wt%, 0.02-0.67wt%, 0.98-4.76wt% respectively, while Mn ranges from 0.32-1.09wt% with an average of 0.66wt%. The loss on ignition ranges from 1.11-3.11wt% with an average of 2.12wt%.In addition, the ores contain impurities such as CaO, MgO, TiO2 and MnO which exist in considerably negligible amounts. Distribution patterns of the geochemical elements (Wt %) in the samples are plotted in Fig 4.4.1.

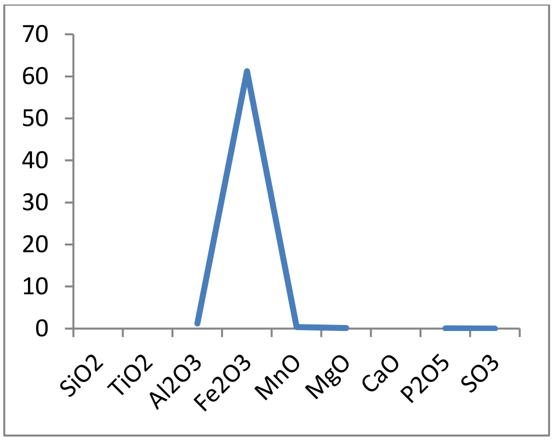

Figure 4.7(a): Distribution pattern of geochemical elements (wt%) in Sample JD1

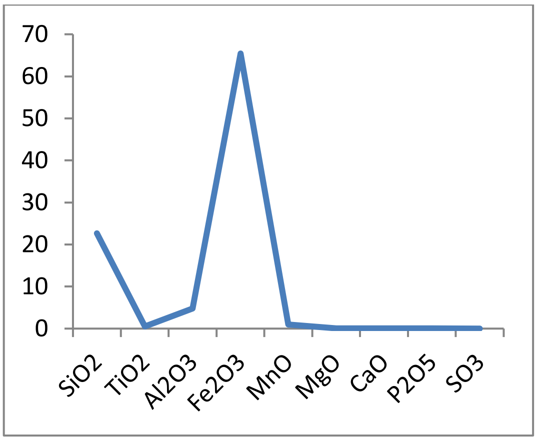

Fig 4.7(b): Distribution pattern of geochemical elements (wt%) in Sample JD2

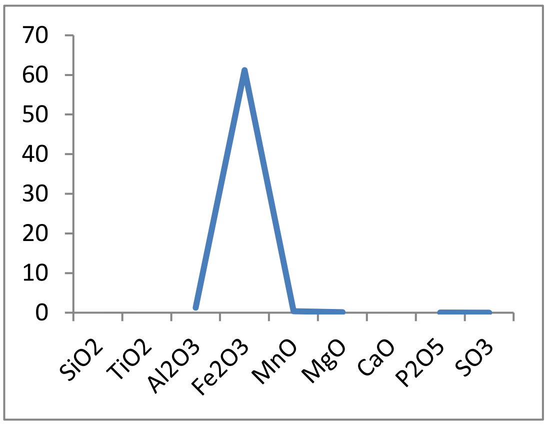

Figure 4.7(c): Distribution pattern of geochemical elements (wt%) in Sample JD3

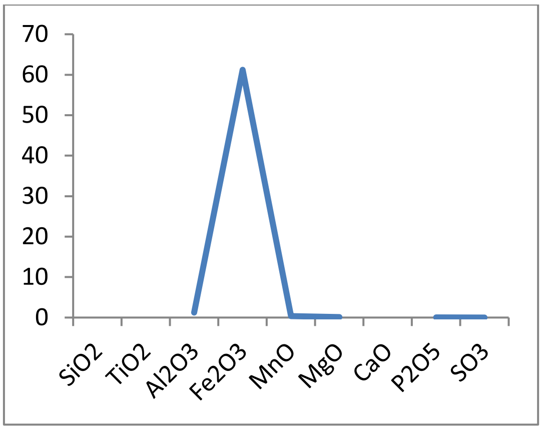

Figure 4.7(d): Distribution pattern of geochemical elements (wt%) in Sample JD4

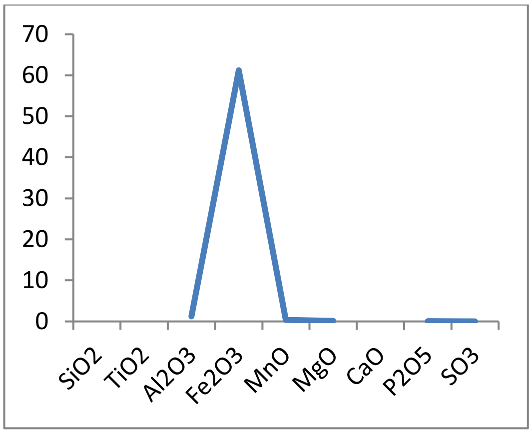

Figure 4.7(e): Distribution pattern of geochemical elements (wt%) in Sample JBL1

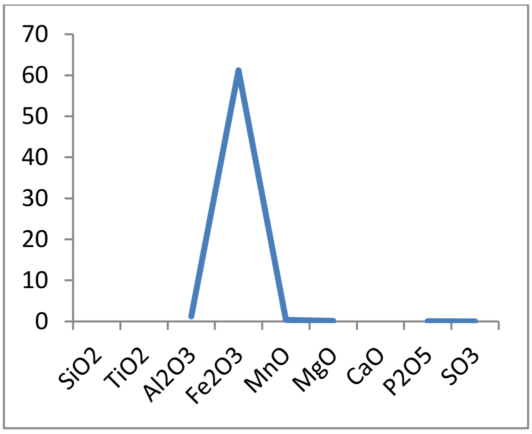

Figure 4.7(f): Distribution pattern of geochemical elements (wt%) in Sample JBL2

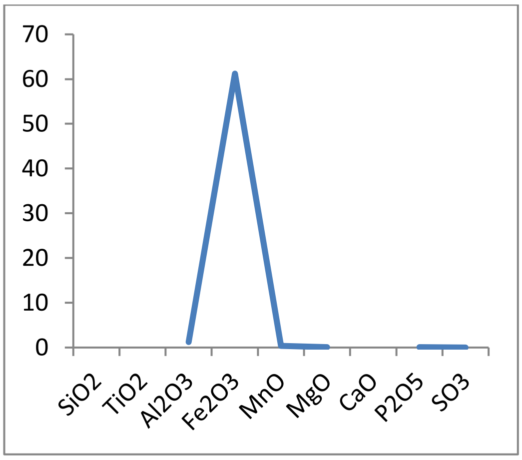

Figure 4.7(g): Distribution pattern of geochemical elements (wt%) in Sample JBL3

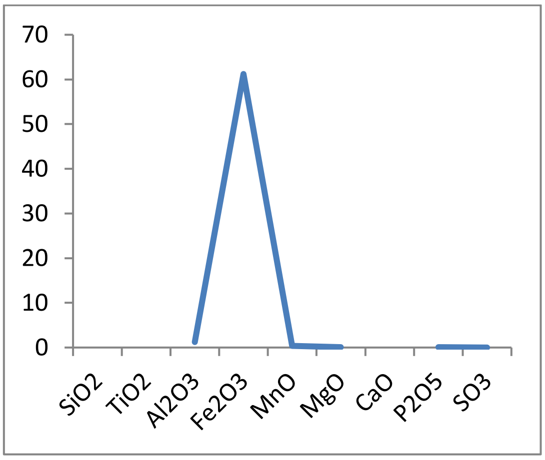

Figure 4.7(h): Distribution pattern of geochemical elements (wt%) in Sample JBL4

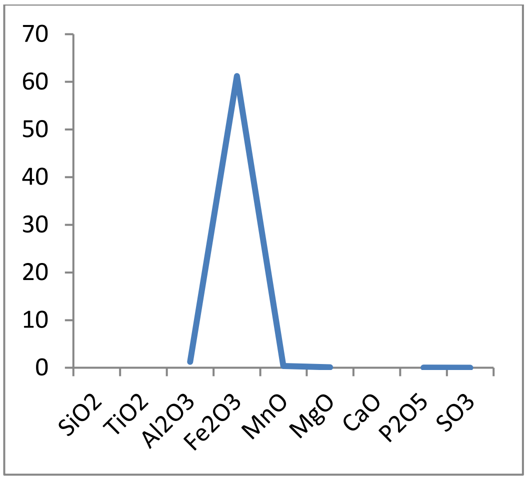

Figure 4.7(i): Distribution pattern of geochemical elements (wt%) in Sample JK1

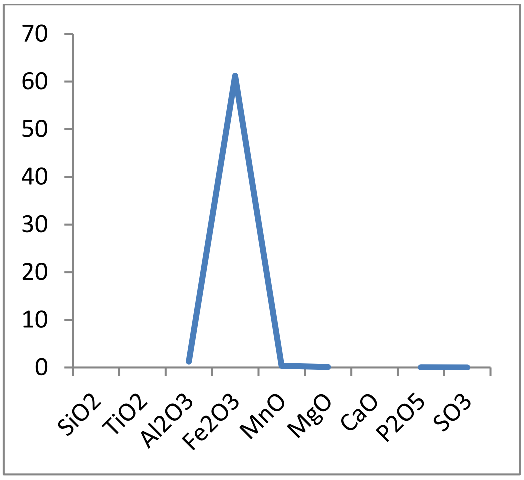

Figure 4.7(j): Distribution pattern of geochemical elements (wt%) in Sample JK2

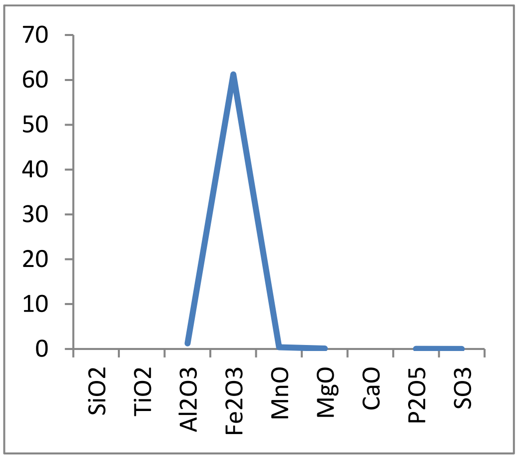

Figure 4.7(k): Distribution pattern of geochemical elements (wt%) in Sample JK3

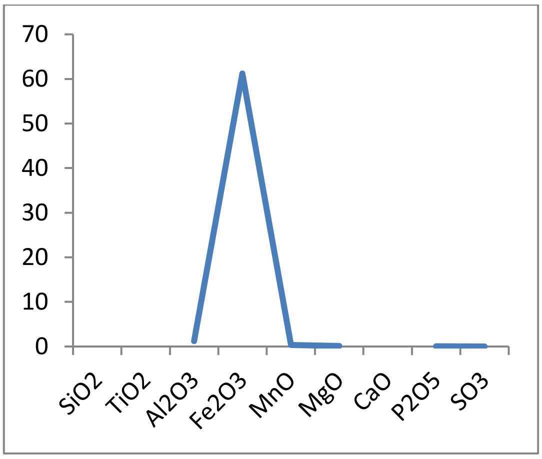

Figure 4.7(l): Distribution pattern of geochemical elements (wt%) in Sample JK4

4.9.2 Beneficiation

Very low grade Iron ore cannot be used in metallurgical plants and needs to be upgraded to increase the iron content and reduce the gangue content. A process adopted to upgrade ore is called Beneficiation. Iron ore is up graded to higher iron content through concentration. Iron ore is being beneficiated all round the world to meet the quality requirement of Iron and Steel industries. However, each source of Iron ore has its own peculiar mineralogical characteristics and requires the specific beneficiation and metallurgical treatment to get the best product out of it. The choice of the beneficiation treatment depends on the nature of the gangue present and its association with the ore structure. Several techniques such as washing, jigging, magnetic separation, advanced gravity separation and flotation are being employed to enhance the quality of their on ore .The aim of this research work is to investigate the possibility of using magnetic separation methods to produce iron ore concentrate that could be used as a charge quality in Nigerian steel plants. The result of the beneficiation carried out using magnetic method is presented below

Sample JD1

Table: 4.9.2(a) Beneficiation result for JD1

Product	weight (%)(g)	Assay (%)	Recovery (%)	Ratio of concentrate	Enriched Ratio	Metal content (g)
Feed	200	66.88	100	1:0	1:0	133.37
Concentrate	124.5	89.17	92	1:3	1:6	150.02
Tailings	69.0	17.0	7.2	0:2	2:9	11.73

Sample JD4

Table: 4.9.2(b) Beneficiation result for JD4

Product	weight (%)(g)	Assay (%)	Recovery (%)	Ratio of concentrate	Enriched Ratio	Metal content (g)
Feed	200	67.11	100	1:0	1:0	134.22
Concentrate	142	90.05	93	1:3	1:4	127.87
Tailings	39	15.8	6.2	0:2	5:1	6.16

Sample JBL1

Table: 4.9.2(c) Beneficiation result for JBL1

Product	weight (%)(g)	Assay (%)	Recovery (%)	Ratio of concentrate	Enriched Ratio	Metal content (g)
Feed	200	66.7	100	1:0	1:0	133.4
Concentrate	170.5	84.0	92.8	1:3	1:2	143.22
Tailings	27.5	18.2	4.5	0:3	7:3	5.01

Sample JBL4

Table: 4.9.2(d). Beneficiation result for JBL4

Product	weight (%)(g)	Assay (%)	Recovery (%)	Ratio of concentrate	Enriched Ratio	Metal content(g)
Feed	200	59.11	100	1:0	1:0	118.22
Concentrate	183.5	81.17	91.9	1:4	1:1	148.64
Tailings	15.0	14.5	2.1	0:3	13:3	2.175

Sample JK1

Table: 4.9.2(e). Beneficiation result for JK1

Product	weight (%)(g)	Assay (%)	Recovery (%)	Ratio of concentrate	Enriched Ratio	Metal content(g)
Feed	200	60.13	100	1:0	1:0	120.26
Concentrate	189	78.0	91	1:3	1:1	147.42
Tailings	0.9	18.0	2.5	0:3	22:2	1.62

Sample JK4

Table: 4.9.2(f). Beneficiation result for JK4

Product	weight (%)(g)	Assay (%)	Recovery (%)	Ratio of concentrate	Enriched Ratio	Metal content (g)
Feed	200	61.22	100	1:0	1:0	122.44
Concentrate	184	74.5	93	1:2	1:1	137.08
Tailings	13.5	19.0	6.0	0:3	14:8	2.565

4.9.3 Discussion of Beneficiation Result

Results obtained from processing Bida Basin iron ore using Magnetic Separation as seen on the tables in Fig. 4.5.1-4.5.6. The magnetic Separation for JD1 gave a mass of concentrate to be 124.5Kg with tailing 69.0 kg and a recovery of 92% for the concentrate and 7.2% for the tailings. The magnetic Separation for JD4 gave a mass of concentrate to be 142Kg with tailing 39 kg and a recovery of 93% for the concentrate and 6.2% for the tailings. The magnetic Separation for JBL1 gave a mass of concentrate to be 170.5Kg with tailing 27.5 kg and a recovery of 92.8% for the concentrate and 4.5% for the tailings. The magnetic Separation for JBL4 gave a mass of concentrate to be 183.5Kg with tailing 15.0 kg and a recovery of 91.9% for the concentrate and 2.1% for the tailings. The magnetic Separation for JK1 gave a mass of concentrate to be 189Kg with tailing 0.9kg and a recovery of 91% for the concentrate and 2.5% for the tailings. The Magnetic Separation for JK4 gave a mass of concentrate to be 184Kg with tailing 13.5 kg and a recovery of 93% for the concentrate and 6.0% for the tailings. From this it can be seen that more quantity of Iron Ore was recovered in the Magnetic Separation. This implies that the quantity by mass of Concentrate obtained using Magnetic Separation method is high.

Table 4.9.3(a): Iron content (%) in raw iron samples (before beneficiation) and iron content in beneficiated samples

Sample Label	Iron content (%) in raw samples (before beneficiation)	Iron content(%) in Beneficiated samples
JD1	66.80	75.01
JD4	60.11	63.94
JBL1	66.70	71.61
JBL4	59.11	74.30
JK1	60.13	73.50
JK4	61.22	68.54

The iron content in the raw samples for samples obtained from Doko area(JD1 and JD4)on an average is 63.46% while the iron content of beneficiated samples from the same location on average is 59.73%.The iron content in the raw samples for samples obtained from Bida-Lemu road area(JBL1 and JBL4)on an average is 62.91% while the iron content of beneficiated samples from the same location on average is 72.96%.The iron content in the raw samples for samples obtained from Kutigi area(JK1 and JK4)on an average is 60.68% while the iron content of beneficiated samples from the same location on average is 71.02%.

CHAPTER FIVE

5.1 CONCLUSION AND RECOMMENDATION

5.2 Conclusion

The result of this study has shown that the ironstone at Bida basin contains high percentage of iron oxide in the form of hematite which ranges from 59.11wt%-66.88wt% with an average of 64.05wt% and it could be described as a high grade ore. A ternary plot of SiO2; FeO + MnO; Fe2O3, used to determine the facies types indicates that the ironstone is of magnetite-silicate facies. A ternary plot of Fe-Mn-(Cu+Zn)*10 plotted for the ironstone in the study area indicated a submarine hydrothermal origin for the analyzed samples. From the XRD results, the dominant iron-bearing mineral is the hematite which is most abundant in sample JBL3 at 71% hematite.

The iron content in the raw samples for samples obtained from Doko area(JD1 and JD4)on an average is 63.46% while the iron content of beneficiated samples from the same location on average is 59.73%.The iron content in the raw samples for samples obtained from Bida-Lemu road area(JBL1 and JBL4)on an average is 62.91% while the iron content of beneficiated samples from the same location on average is 72.96%.The iron content in the raw samples for samples obtained from Kutigi area(JK1 and JK4)on an average is 60.68% while the iron content of beneficiated samples from the same location on average is 71.02%. The magnetic separation result meets the requirement of 62-65% Fe (minimum) and 3.0% (maximum) silica+ Alumina + titanium oxide in the production of Nigerian iron and steel in Steel Industries

5.2 Recommendation

The dominance of oil on the Nigerian economy has not helped matters, therefore, a proper knowledge of the geology and accurate inventory of the potential of ironstone in the Bid Basin and the documentation of this work/information in the form of thesis is very necessary to update and contribute to the knowledge of Bida Basin and possibly attract public and private sector investors to the deposit of ironstone sector of the Niger State economy and that of our beloved country, Nigeria, which in turn should lead to the establishment of small and medium scale enterprises. Such enterprises will resuscitate economic activities that will lead to economic growth, employment generation, poverty reduction and social tranquility.

REFERENCE

Abimbola, F. A. (1997). Petrographic and paragenetic studies of the Agbaja ironstone formation, Nupe Basin, Nigeria. *Journal of African Earth Science* 25, 169-181.

Adekoya, J. A. (1996). The geology and geochemistry of the Maru Banded Iron-Formation, Northwestern Nigeria. *Journal of African earth sciences*, 27(2)24-257.

Adeleye D. R. (1973). Origin of ironstone an example from the middle Niger valley; Elizabethan pub.co Lagos Nigeria, 283-287.

Adeleye, D. R. (1974). Sedimentology of the fluvial Bida Sandstone (Cretaceous) *Nigeria. Sedimentary Geology* (12) pp 1-24

Adeniyi, J. O. (1985). Ground total magnetic intensity in parts of the Nupe Basin and the 67–78.adjacent basement complex, Niger State, Nigeria. *Nigerian Journal of Applied Science* (3).

Barley, M. E., Pickard A. L., Hagemann S. G. & Folkert S. L. (1999). Hydrothermal origin for the 2 billion year old Mount Tom Price giant ore deposit, Hamersley Province, Western Australia. *Mineralium Deposita* 34, 784-798.

Barnes, J. W. (1989). Ores and minerals: introducing economic geology. Open University Press, Milton Keynes — Philadelphia. 181.

Bekker, A., Planavsky, N. J., Krapež, B., Rasmussen, B., Hofmann, A., Slack, J. F., Rouxel, O. J. & Konhauser, K. O. (2014). *Iron Formations: Their Origins and Implications for Ancient Seawater Chemistry. In: Treatise on Geochemistry* (Second Edition) 9, 561–628.

Benkhell, J. (1989). The origin and evolution of the cretaceous Benue Trough, Nigeria. *Journal of African Earth science*, 8, 251-272.

Blatt, H. (1982). *Sedimentary petrology. Numerious figs and tables*: San fransisco: Freeman, 12, 564.

Boggs, S. Jr. (2006). *Principles of Sedimentology & Stratigraphy*, 4th edition, Prentice Hall, 662 p.

Bonatti E. (1975). Metallogenesis at oceanic spreading centers: *Annual review of earth & planetary science*, 3, 401-403.

Bottke, H. (1981). Lagersta¨ttenkunde des Eisens. Verlag Glu¨ckauf GmbH, Essen, 75–97.

Danbatta. U. (1999). The structural frame work underlying the metamorphic evolution of the Kazaure schist belt NW Nigeria; *Global journal of geological sciences*. 4, 35- 37.

Dobbins M. S. & Burnet G. (1982). “Production of iron ore concentration from the iron-rich fraction of power plant fly ash, “*Resources and conservation*, 9, 231-242.

Edwards, R. & Atkinson, K. (1986). *Ore Deposit Geology and its influence on mineral exploration*. Chapman and Hall, London.

Evans P. R. (1967). Palynological examination of a lower cretaceous (Albian) siltstone from the Gove Peninsula: in Dodson RG, 1967. Coal at Gove Peninsula, NT. Bureau of mineral. *Resources, Geology and Geophysics*, Australia, Record 1967/087, Appendix 3.

Evans, A. M. (1993). Ore Geology and Industrial Minerals (third Edition). *Blackwell Science*. 38 pp.

Goro, A. I., Salihu, H. D., Jibrin, B. W., Waziri, N. M. & Idris-Nda, A. (2014). Characterization of a massive sandstone interval: Example from DOKO member of Bida Formation, northernBida Basin, Nigeria. *Universal Journal of Geoscience* 2 (2), 53-61.

Gross G. A. (1970). Natural and occurrence of iron ore deposits: in United Nations, Departments of Economic and social Affairs (editors) survey of world iron ore resources, occurrence and appraisal. United Nations, New York, 13-31.

Gross G. A. (1993). Industrial and genetic models for iron ore in iron-formations: In Kirkham, R. V., Sinclair, W. D., Thorpe, R. I. and Duke, J. M. (editors) '*Mineral Deposits Modelling*'. *Geological Association of Canada*, 40, 151-170.

Hasan J. & Onimesi J. (2019). Geochemical and petrogenetical characterisation of ironstone deposit from Agbaje Formation Bida Basin Nigeria; http// www.researchgate publication.

Hitzman M. W., Oreskes, N. & Einaudi M. (1992). Geological characteristics and tectonic setting of Proterozoic iron oxide (Cu-U-Au-REE) deposits. *Precambrian Research* 58, 241-287.

Ibrahim, G. (2002). Sedimentary facies of iron-formation. *Economic. Geology*, 49, 325-328.

Imrana, A. & Haruna I. V. (2017). Geology, Mineralogy & Geochemistry 0f KotonKarfe Oolitic Iron Ore Deposit, Bida Basin. Kogi State, Nigeria; *International journal of scientific & technology research*, 6, (08) 191-203.

James H. L. (1983). *Distribution of banded iron formation in space and time*. In: Trendall, A. F., and Morris, R. C. (Eds.), Iron- *Formation: Facts & Problems. Amsterdam*: Elsevier, pp.471-490.

James, H. L. (1966). Chemistry of Iron-Rich Sedimentary Rocks: Data of Geochemistry, 6th edition: *US Geological Survey Professional Paper* 440-W.

James, H. L. (1982), Sedimentary Facies of Iron-formation. *Economic Geology*, 49, 235-293.

Jones, N. O. (1955). Geological report on the Mucketty manganese deposit. *Bureau of Mineral Resources, Geology and Geophysics*, Australia, Record 1995/120.

Katrak, F. E. (2008). Future of Iron and steel. In K. H. J. Buschow (Ed), *Encyclopedia of materials: science & technology*, 23, 4292-4295.

Khan. M. A. & Ungar, A. (1996) Comparative study of ironstone in Bida Basin. *Geological society of Nigeria special publication* 50, 180-185.

Kimberely, M. M. (1989a). Nomenclature for iron formations. *Ore Geology Reviews* 5, 1-12.

Kimberely, M. M. (1989b). Exhalative origins of iron formations. *Ore Geology Review* 5, 12-145.

Kimberley, M. M. (1994). Debate about ironstone: has solute supply been surficial weathering, hydrothermal convection, or exhalation of deep fluids?. *Terra Nova* 6, 116–132.

Klein, C. & Beukes N. J. (1993). Sedimentology and geochemistry of the glaciogenic Late Proterozoic Rapitan iron-formation in Canada. *Economic Geology* 88, 542–565.

Klemic H, James, H. L. & Eberlein, D. G. (1973). Iron: in Brobst DA and Pratt WP (editor) '*United State Mineral resource*.' US Geological Survey Professional Paper 820, 291-306.

Kogbe, C. A. (1978). Origin and Composition of the Ferruginous oolites and laterites of NW Nigeria. *Geologische Rundscheu* 67, 262-274.

Ladipo, K. O., Akande, S. O. & Muck, A. (1994). Genesis of ironstones from the Mid-Niger Sedimentary basin: evidence from sedimentological, ore microscopic and geochemical studies. *Journal of Mining and Geology*, 30, 161-168.

Maynard, J. B. (1991). Iron: Syngenetic deposition controlled by the evolving ocean-atmosphere system. In: Force, E., Eidel, J. J., Maynard, J. B. (Eds.), Sedimentary and diagenetic mineral deposits: A basin analysis approach to exploration: El Paso, Texas, *Society of Economic Geologists, Reviews in Economic Geology* 5, pp. 141–145.

Morris, R. C. (1988). BIF-hosted iron ore deposits-Hamersley style. AGSO *Journal of Australian Geology and Geophysics* 17(4), 207-211.

Mücke, A. & Farshad, F. (2005). Whole-rock & mineralogical composition of Phanerozoic ooidalironstones: comparison & differentiation of types and subtypes. *Ore Geology Reviews*. 26,227– 262.

Mucke, A. (1994). Post-diagenetic ferruginisation of sedimentary rocks (sandstone, oolitic ironstone, kaolinsand bauxite) including a comparative study of the redding of red beds. In: *Development of Sedimentology Diagenesis,* 4 (Edited by Wolf, K. and Chilingarian, G. V.) 361-423. Elsevier, Amsterdam.

Mucke, A. (1999). The Nigerian Manganese-rich Iron-formations & their host rocks from sedimentation to metamorphism: *Journal of African Earth Sciences*, 41, 407-436.

Mucke, A., Annor, A. & Neuman, U. (1996). The Algoma type iron-formations of the Nigerian metavolcano-sedimentary schist belts. *Minerallium deposita* 31, 113-122.

Obaje, N. G, Akinsanpe, O. T., Ojo, G. A. & Akande, W. G. (2019). Revise Stratigraphy of Bida Basin, Nigeria; *Journal of African earth science*, 151, 67-81.

Ojo, O. J. & Akande, S. O. (2012). Facies Analysis and Paleo environments of the UpperCretaceous sediments in the Share - Lafiagi area, northen Bida Basin. *Nigerian Mining and Geosciences Society (NMGS)*, 10, 111-126.

Ojo, S. B. & Ajakaiye, D. E., (1989). Preliminary interpretation of gravity measurements in the Mid-Niger Basin area, Nigeria. In; Kogbe, C.A.(Ed), Geology of Nigeria. 2nd edition, Elizabethan Publishers, Lagos, 347-358.

Ojo, S. B. & Ajakaje, D. E. (1989). Preliminary interpretation of gravity measurement in the middle Niger Basin area, Nigeria. In: Kogbe, C.A. (Ed), Geology of Nigeria 2nd edition, Elizabethan Publishers, Lagos, 347-358.

Ojo. S. B. (1984). Middle Nigeria Basin Revisited, Magnetic constraints on gravity interpretations. Nigerian mining and Geosciences society conference, Nsukka, Nigeria, Abstract. 52-53.

Okosun, E. A., Goro, A. I., Olobaniyi, S. B., Shekwolo, P. D. & Nwosu, J. E. (2007). Stratigraphy of the Bida Formation, Bida Basin, Nigeria. *Borno Journal of Geology*. 4(2), 21-37.

Onodoku, U. S., Edwin, O., Isah, G. & Salisu, H. D. (2017). Palynological Evidence of a Campanian-Maastrichtian Age of the Central Bida Basin, Nigeria: Implication for Paleoenvironment, Paleoclimate and Hydrocarbon Prospectivity; Minna *Journal of Geosciences* (MJG), 1 (1), (165 – 178).

Oyewola, O. M. (2011). On wind speed pattern & energy potential in Nigeria, *Energy policy, Elsevier*, 39(5), 2501-2506.

Petránek, J. & Van Houten, F. B. (1997). Phanerozoic ooidal ironstones. Czech *Geological Survey Special paper* 7, 71.

Petters, S. W. (1978). Middle cretaceous paleoenvironments & biostratigraphy of the Benue Trough, Nigeria. *Geology society of America Bulletin* 89, 151-154.

Pollard. P. J. (2000). Evidence of a magmatic fluid & metal source for Fe-oxide Cu-Au mineralisation: In Porter, T. M. (editor). *Hydrothermal iron-oxide copper gold and related ore deposits:* a global prospective. Australian Mineral Foundation, Adelaide 27-41.

Powell, C. A., Oliver, N. H. S., Li, Zheng-Xiang., Martin, D. B. & Ronaszecki, J. (1999). Synorogenic hydrothermal origin for giant Hamersley iron oxide ore bodies. *Geology*, 27(2), 175-178.

Pratt, R. (1978). Australian use of iron oxide minerals for purpose other than iron & steel making. *Australian Mineral Industry Quarterly*. 31, 166-176.

Pratt, R. (1993). *Austraila's iron ore resources*. Resource report. Bureau of Resource Sciences, Canberra.

Rahaman, M. A. O., Fadiya, S. L., Adekola, S. A., Coker, S. J., Bale, R. B., Olawoke O. A., Omada, I. J., Siehl, A. & Thein, J. (1989). Minette-type ironstones. In T.P. Young & W.E.G. Taylor (eds), Phanerozoic Ironstones. *Geological Society London, Special Publication*, 46, 175–93.

Robb, L. (2004). *Introduction to ore-forming processes*. 247-266. Black Well Scientific Publication, Oxford.

Rollinson, H. (1993). Using geochemical data: evaluation, presentation, interpretation. *Longman Group*, England, UK, 133-303.

Schull, T. J. (1988). Rift basin of interior sudan: petroleum exploration and discovery, *American Association of Petroleum Geologisit bulletin*, Tulsa, 72, 1128-1142.

Siehl, A., & Thein, J. (1989). Minette-type ironstones. In: Young, T.P., Taylor, W. E. G. (Eds.), Phanerozoic Ironstones. *Geological Society of London, Special Publication* 46, 175–193.

Sokar. T. (1990). Concentration of trace metals (lead iron copper and zinc) in crops harvested in some oil prospecting locations in River state, Nigeria. *Geology society London, Special Publication*, 3, 205-208 pp.

Stanton. R. L. M. (1972). *Metal Deposits: Ore petrology*, Hill New York, 13, 714.

Sully, A. H. (1987). *Manganese*: In Parker, S. P. (editor). McGraw Hill Encyclopedia of science & technology. McGraw Hill, New York, 10, 362-365.

Taylor, D., Dalstra, H. J., Harding, A. E., Broadbent, G. C. & Barley, M. E. (2001). Genesis of hih-grade hematite ore bodies of the Hemerslay province, *Western Australia. Economic Geology* 96(4), 837-873.

Trendall, A. F. & Blocklay, C. (1970). Iron-Formation: facts and Problems, *Elsevier Science Publishers* B.V.

Udensi, E. E. & Osazuwa, I. B. (2004). Spectral determination of depths to magnetic rocks under the Nupe Basin, Nigeria. *Nigerian Association of Petroleum Explorationists Bulletin* (17) 22–27.

Van Houten, F. B. & Hou, Hong-Fei., (1990). Stratigraphic and palaeogeographic distribution of '*Palaeozoic oolitic ironstones: in McKerrow,* W. S. *& Scotese,* C. R. *(editors) Palaeozoic Palaeogeography & Biogeography'*. *Geological Society Memoir* 12, 87-93.

Van Houten, F. B. (1992). Review of Cenozoic ooidal ironstones. *Sedimentary Geology* 78, 101–110.fkv8s7

Young, T. P. (1989). Phanerozoic ironstones: an introduction & review: *Geological society special publication*, 46, 9-25.